

Linking new genes to an odontogenesis *TP63*-mediated gene regulatory network that is
peripheral to jaw morphogenesis

College of Graduate and Postdoctoral Studies

Degree of Master of Science

Department of Anatomy and Cell Biology

University of Saskatchewan, Saskatoon, Saskatchewan, Canada

Nasim Rostampour

© Copyright Nasim Rostampour, February 2018. All rights reserved.

PERMISSION TO USE

In presenting this thesis/dissertation in partial fulfillment of the requirements for a Postgraduate degree from the University of Saskatchewan, I agree that the Libraries of this University may make it freely available for inspection. I further agree that permission for copying of this thesis/dissertation in any manner, in whole or in part, for scholarly purposes may be granted by the professor or professors who supervised my thesis/dissertation work or, in their absence, by the Head of the Department or the Dean of the College in which my thesis work was done. It is understood that any copying or publication or use of this thesis/dissertation or parts thereof for financial gain shall not be allowed without my written permission. It is also understood that due recognition shall be given to me and to the University of Saskatchewan in any scholarly use which may be made of any material in my thesis/dissertation.

DISCLAIMER

Reference in this thesis/dissertation to any specific commercial products, process, or service by trade name, trademark, manufacturer, or otherwise, does not constitute or imply its endorsement, recommendation, or favoring by the University of Saskatchewan. The views and opinions of the author expressed herein do not state or reflect those of the University of Saskatchewan, and shall not be used for advertising or product endorsement purposes.

Requests for permission to copy or to make other uses of materials in this thesis/dissertation in whole or part should be addressed to:

Head of the Department of Anatomy & Cell Biology

107 Wiggins Rd.

University of Saskatchewan

Saskatoon, Saskatchewan, SK S7N 5E5

Canada

OR

Dean

College of Graduate and Postdoctoral Studies

University of Saskatchewan

116 Thorvaldson Building, 110 Science Place

Saskatoon, Saskatchewan S7N 5C9

Canada

ABSTRACT

Despite that teeth and jawbones can develop and evolve independently of each other, the genetic processes that independently regulate cranial and dental morphogenesis remain unclear. Previous microarray screens indicated that a *TP63*-mediated gene regulatory network is integral to odontogenesis but peripheral to jaw morphogenesis.

Here, I characterized the expression of four genes flagged by our lab's previous microarray screens, comparing embryonic wild-type and *TP63*-null (*TP63*^{-/-}) mutant mouse mandible prominences. I hypothesized that in the normal dental epithelium, *TP63* up-regulates *Fermt1* and *Pltp* and down-regulates *Cbhl1* and *Krt8*.

I validated the expression domains of these genes in *TP63*^{-/-} mutant and wild-type mice using RNA *in-situ* hybridization on paraffin tissue sections at two stages, E11.5, just after odontogenesis begins, and at E13.5, just after odontogenesis arrests in the *TP63*^{-/-} mutant. My *in situ* results validated our lab's previous microarray screens. My work revealed that *Fermt1* is expressed in wild-type oral epithelium and dental epithelium, and that *Pltp* is expressed in dental epithelium. Compared to wild-type littermates, in *TP63*^{-/-} mice, *Fermt1* and *Pltp* expression intensity in the dental epithelium was decreased. *Cbhl1* was not expressed in wild-type dental epithelium, although it expressed intensely in the dental epithelium of *TP63*^{-/-} littermates. *Krt8* was expressed in the dental epithelium of both wild-type and *TP63*^{-/-} embryos, with increased intensity in the *TP63*^{-/-} mice. In sum, my results largely supported my hypothesis.

As such, I propose that *Fermt1*, *Pltp*, *Cbhl1*, and *Krt8* belong to a *TP63*-mediated gene regulatory network and co-regulate odontogenesis by mediating cell adhesion, cell signaling, and epithelial-mesenchymal interactions at early stages of tooth development.

ACKNOWLEDGEMENTS

First and foremost, I would like to express my deepest gratitude to my supervisor, Dr. Julia Boughner, for accepting me as her Master student and continuous support of my Master study. She has been patient and supportive since the days I began working on my thesis, I wish to thank her.

My thesis Committee guided me through these two years, I am so grateful for their encouragement, advice, and expertise. My sincere thanks go to Dr. Patrick Krone and Dr. Brian Eames.

I would also like to thank the College of Medicine, the Department of Anatomy and Cell Biology, and the University of Saskatchewan through the CIHR-THRUST fellowship that have supported me and allowed me to do this research. I would also like to thank NSERC for supporting my thesis research via a Discovery Grant to Dr. Boughner.

Also thank our animal care expert, Carmen Whitehead, for her amazing ability to take care of my project's animal needs throughout the program.

Last but not the least, I like to express my profound gratitude to my parents, sister and brother: thanks for pushing me all along this journey. This accomplishment would not have been possible without your encouragement and unwavering support.

TABLE OF CONTENTS

PERMISSION TO USE.....	i
ABSTRACT.....	iii
ACKNOWLEDGEMENTS.....	iv
LIST OF TABLES.....	vii
LIST OF FIGURES.....	viii
LIST OF ABBREVIATIONS.....	ix
CHAPTER 1 - INTRODUCTION.....	1
1.1 Molecular biology of odontogenesis exclusive of jaw morphogenesis.....	1
1.2 The developmental stages of tooth morphogenesis in mammals.....	2
1.3 The integral role of <i>TP63</i> in initiating odontogenesis.....	4
1.4 Thesis research questions and objectives.....	7
1.4.1 Adding new genes to a <i>TP63</i> -mediated gene regulatory network active during mouse embryonic development.....	7
1.4.2 Mapping the expression of four new genes at the beginning of tooth initiation and the later bud stage of tooth development.....	9
CHAPTER 2 - MATERIALS AND METHODS.....	10
2.1 Study methodology: Overview.....	10
2.2 Study materials.....	10
2.2.1 Mice.....	10
2.2.2 Phenotyping.....	11
2.3 DNA extraction and genotyping.....	11
2.4 Embryo processing and sectioning.....	15
2.5 Hematoxylin and Eosin staining.....	18

2.6 RNA <i>in situ</i> hybridization.....	20
2.6.1 Designing RNA probes.....	20
2.6.2 Probe synthesis.....	21
2.6.3 <i>in situ</i> hybridization.....	24
2.7 Gene expression documentation.....	27
CHAPTER 3 - RESULTS.....	28
3.1 Digoxigenin-labeled RNA probe synthesis results.....	28
3.2 The expression of <i>TP63</i> , <i>Shh</i> , and four novel genes (<i>Fermt1</i> , <i>Pltp</i> , <i>Cbln1</i> , and <i>Krt8</i>) in tooth organ and jaw at E13.5.....	30
3.3 The expression of <i>TP63</i> , <i>Shh</i> , and four novel genes (<i>Fermt1</i> , <i>Pltp</i> , <i>Cbln1</i> , and <i>Krt8</i>) in tooth organ and jaw at E11.5.....	34
3.4 Negative controls using sense probes.....	36
CHAPTER 4 - DISCUSSION AND CONCLUSIONS.....	37
4.1 The importance of the <i>TP63</i> transcription factor and its gene regulatory network in the oral dentition in mammals.....	37
4.2 Putative roles of these four new candidate genes in a tooth-specific <i>TP63</i> gene regulatory network.....	39
CHAPTER 5 - REFERENCES.....	46
Appendix A.....	53

LIST OF TABLES

Table 1. Results of microarray analysis showing the differences in gene expression caused by the null mutation of TP63 during odontogenesis	8
Table 2. List of PCR primers that were designed and validated by Jackson Laboratories and purchased from Sigma.....	12
Table 3. Each PCR reaction mixture	13
Table 4. Thermocycler program.....	14
Table 5. Tissue dehydration steps.....	16
Table 6. Tissue processor program.....	17
Table 7. H & E staining protocol.....	19

LIST OF FIGURES

Figure 1. The four distinct stages of odontogenesis: (A) dental lamina formation at E10.5, (B) bud stage at E13.5, (C) cap stage at E14.5, and (D) bell stage at E18.5.	4
Figure 2. (A) Neonatal Brdm2 mouse, showing (<i>TP63</i> ^{-/-}) phenotype, in comparison to (<i>TP63</i> ^{+/+}). (B-D) Comparing mandible shapes among (B) <i>TP63</i> wild-type (<i>TP63</i> ^{+/+}), (C) <i>TP63</i> heterozygote (<i>TP63</i> ^{+/-}) and (D) <i>TP63</i> -null fetuses (E18) (<i>TP63</i> ^{-/-})	6
Figure 3. UV light view of a typical PCR agarose gel	15
Figure 4. UV light view of agarose gel of all six genes after DNA plasmids linearization	22
Figure 5. UV light view of an agarose gel showing all six genes after DNA plasmid purification	23
Figure 6. UV light view of an agarose gel showing antisense probes for six genes.....	29
Figure 7. UV light view of an agarose gel showing sense probes for six genes.....	29
Figure 8. Coronal view of mouse head (A), showing tooth organ at bud stage and (B) <i>TP63</i> expression at E13.....	31
Figure 9. RNA <i>in situ</i> hybridization at E13.5 with expression of (A, B) <i>Shh</i> , (C, D) <i>TP63</i> , (E, F) <i>Fermt1</i> , (G, H) <i>Pltp</i> in dental epithelium in <i>WT</i> and <i>TP63</i> ^{-/-} mice.....	32
Figure 10. RNA <i>in situ</i> hybridization at E13.5 with expression of (A, B) <i>Shh</i> , (C, D) <i>TP63</i> , (E, F) <i>Cbln1</i> , (G, H) <i>Krt8</i> in dental epithelium in <i>WT</i> and <i>TP63</i> ^{-/-} mice.....	33
Figure 11. RNA <i>in situ</i> hybridization at E11.5 with expression of (A, B) <i>Shh</i> , (C, D) <i>TP63</i> , (E, F) <i>Fermt1</i> , (G, H) <i>Pltp</i> in dental epithelium in <i>WT</i> and <i>TP63</i> ^{-/-} mice.....	34
Figure 12. RNA <i>in situ</i> hybridization at E11.5 with expression of (A, B) <i>Shh</i> , (C, D) <i>TP63</i> , (E, F) <i>Cbln1</i> , (G, H) <i>Krt8</i> in dental epithelium in <i>WT</i> and <i>TP63</i> ^{-/-} mice.....	35
Figure 13. RNA <i>in situ</i> hybridization at E13.5, use of <i>sense</i> RNA probes for <i>Fermt1</i> , <i>Pltp</i> , <i>Cbln1</i> , and <i>Krt 8</i> in <i>WT</i> mice as a negative control for each probe.....	36
Figure 14. Venn diagram: (A) genes important for mandible and tooth development that do not act within a <i>TP63</i> odontogenic <i>GRN</i> ; versus (B) other genes/ <i>GRNs</i> that regulate odontogenesis; and (C) candidate members of a <i>TP63</i> odontogenic <i>GRN</i>	38

LIST OF ABBREVIATIONS

AP	Alkaline Phosphatase
BMP	Bone morphogenic protein
BM	Basement membrane
Bmp4	Bone morphogenic protein 4
bp	Base pairs
Brdm2	Homozygote mutant of TP63
C	Celcius
Cbln1	Cerebellin 1 Precursor
cDNA	complementary DNA
ddH ₂ O	double-distilled water
DEPC	Diethyl pyrocarbonate
DIG	Digoxigenin
DNA	Deoxyribonucleic acid
E	Embryonic day
E.coli	Escherichia coli
ECM	Extracellular matrix
EDTA	Ethylenediaminetetraacetic acid
EtOH	Ethanol
Fermt1	Fermitin Family Member 1
FGF	Fibroblast growth factor
Fgf8	Fibroblast growth factor 8
GRN	Gene regulatory network
H ₂ O	Water
HCl	Hydrogen chloride
HDL	High-density lipoprotein
ISH	In situ hybridization
Krt8	Keratin 8
LDL	Low-density lipoprotein
LiCl	Lithium chloride
MAB	Maleic acid buffer
MABT	Maleic acid buffer containing Tween 20
MdP	Mandibular prominence
MgCl ₂	Magnesium chloride
mRNA	Messenger ribonucleic acid
Msx1	Msh homeobox 1
NaCl	Sodium chloride

NCBI	National Center for Biotechnology Information
PBS	Phosphate buffered saline
PCR	Polymerase chain reaction
PFA	Paraformaldehyde
Pltp	Phospholipid Transfer Protein
RNA	Ribonucleic acid
RT	Room temperature
Shh	Sonic hedgehog
SOC	Super optimised broth with the addition of glucose
TAE	Tris-acetate-EDTA
TBE	Tris/Borate/EDTA
TNF	Tumor necrosis factor
TP53	Tumor protein 53
TP63	Tumor protein 63
TP63 ^{-/+}	Heterozygote
TP63 ^{+/+}	Wild-type
TP73	Tumor protein 73
Tris	Trisaminomethane
UTR	Untranslated region
UV	Ultra violet
WT	Wild-type
ΔN-p63	TP63 isoform missing N-terminal transactivating domain

CHAPTER 1 - INTRODUCTION

1.1 Molecular biology of odontogenesis exclusive of jaw morphogenesis

In vertebrates, diverse shapes and sizes of teeth and jaws fit and function together; this successful adaption guarantees an individual's feeding and consequently a species' survival (McCollum and Sharpe 2001). Teeth are developmentally and evolutionarily integrated with the jaw structures; yet teeth and jawbones can develop and evolve independently of each other (Rücklin et al. 2012; Paradis et al. 2013). This independence suggests that even though dentitions and jaw skeletons are strongly integrated, there is a genetic process that is vital to odontogenesis but peripheral to jaw morphogenesis. Thus, some genes may be crucial to tooth but not jaw development, and vice-versa.

The genetics of odontogenesis are complex. A large number of genes are responsible for coding growth factors (e.g., Fibroblast growth factor (*FGF*) and Bone morphogenic protein (*BMP*)), signaling molecules (e.g., Sonic hedgehog (*Shh*) and Tumor necrosis factor (*TNF*)), and transcription factors (e.g., Msh homeobox 1 (*Msx1*)) that regulate multiple downstream target genes (Thesleff 2006; Frase et al. 2009). These many genes, as well as their complex interactions, make it challenging to define the molecules and pathways regulating tooth formation, particularly independent of jaw development. Our knowledge of the molecular biology of odontogenesis is based on the targeted mutation of genes such as *Fgf8*, *Bmp4*, *Shh*, and *Msx1* that are critical for both odontogenesis and jaw development. Thus experimental mutation of these genes perturbs both the dentition and the jaw skeleton (Cobourne and Sharpe 2003), making it technically complex to study the genetic processes and pathways that drive odontogenesis distinct from jaw development (Raj and Bougher 2016).

Nonetheless, understanding the conserved gene regulatory network(s) (GRN) that regulates teeth exclusive of jaws is crucial to clarify the factors that synchronize dental and craniofacial development (Paradis et al. 2013). Moreover, this knowledge is important to understand the putative ability for each of these structures - dentition and jaw - to change relative to one another during evolution (Boughner and Halgrimmson 2008).

1.2 The developmental stages of tooth morphogenesis in mammals

Odontogenesis is complex due in part to the highly coordinated epithelial-mesenchymal genetic interactions required to form a tooth (Chatterjee and Boaz 2011). In fact, odontogenesis relies on uninterrupted mesenchymal-epithelial signaling (Thesleff et al. 1991).

The basement membrane (BM) is a thin layer of extracellular matrix (ECM) between dental epithelium and underlying neural crest-derived mesenchyme cells that plays an important role in regulating epithelial-mesenchymal interactions (Thesleff et al. 1991). Also, the extracellular matrix (ECM) between epithelial cells regulates cell interactions during tooth morphogenesis (Fukumoto and Yamada 2005).

More than 100 years ago, the basic stages of tooth morphogenesis were first described (e.g., Owen 1840-1845). From that time and based on all vertebrates studied since, these four distinct stages are similar and consist of: 1) dental placode formation, followed by; 2) bud, then; 3) cap, and finally; 4) bell stage (Fig. 1) (Jernvall and Thesleff 2012). Among the vertebrate model systems that have been used to study the discrete stages and structures of odontogenesis, the mouse is a well-established classical model system. Because of the conserved processes of odontogenesis, data from mouse odontogenesis can be translated to that of other mammalian if not also other vertebrate groups (Thesleff and Ekblom 1984; Chai et al. 1998).

In mice, the first morphological sign of odontogenesis is the thickening of the oral epithelium that happens at embryonic day (E)10.5 (Fig. 1A). At E11.5, dental placodes develop and then forms the primary dental lamina, where the future tooth will form (Thesleff and Tummers 2009; Lumsden 1988). Which they share morphological as well as molecular features with placodes of other ectodermal derivatives, such as hair and nails (Pispa and Thesleff 2003). As the earliest, primary signaling center of the tooth, the dental placode emits signals that help govern tooth bud formation via the localized proliferation of dental lamina cells by E13.5 (Fig. 1B) (Thesleff 2003). One of these important signals is Sonic hedgehog (*Shh*), which is essential to vertebrate tooth development and a highly-conserved marker for odontogenesis (Hardcastle et al. 1998). *Shh* signaling begins very early in tooth development and specifies the odontogenic epithelium in the oral cavity during the initiation of the dental lamina formation (Hu et al. 2013). Later, *Shh* is important for epithelial differentiation and morphogenesis, and promotes epithelial cell movement in the early tooth bud (Li et al. 2016). For the first molar tooth, during the bud stage (E13.5), the dental epithelium invaginates the underlying dental mesenchyme and these epithelium cells divide into two lineages: 1) a single layer of peripheral basal epithelial cells contacting BM, and 2) the stellate reticulum loosely arranged located in the center. (Pansky 1982; Thesleff and Tummers 2009). During the cap stage starting at E14.5 (Fig. 1C), the dental epithelium is in turn invaginated by a group of condensed mesenchymal cells, called the dental papilla, that later gives rise to dentine and dental pulp. The dental epithelium folds and forms a cap-shaped structure called the enamel organ, which covers the dental papilla. The primary enamel knot, another epithelium-derived signaling center, also appears at this stage (Pansky 1982; Thesleff and Tummers 2009). The bell stage starts at E18.5; during this stage and the cap stage (Fig. 1C-D), enamel and dentin are secreted to create the tooth crown (Pansky 1982).

Enamel and dentin are the hard tissues of the tooth. Enamel is secreted by ameloblasts, which are epithelial derivatives, while dentin is secreted by odontoblasts, which are mesenchymal derivatives. Tooth crown size and shape are regulated by the enamel knots, which control where cusps form (Mitsiadis et al. 2010). After crown formation is complete, root formation starts as still-secreting odontoblasts and ameloblasts migrate away from the occlusal surface of the crown. By the time the tooth emerges into the oral cavity, the roots have reached their full length (Pansky 1982; Thesleff and Tummers 2009).

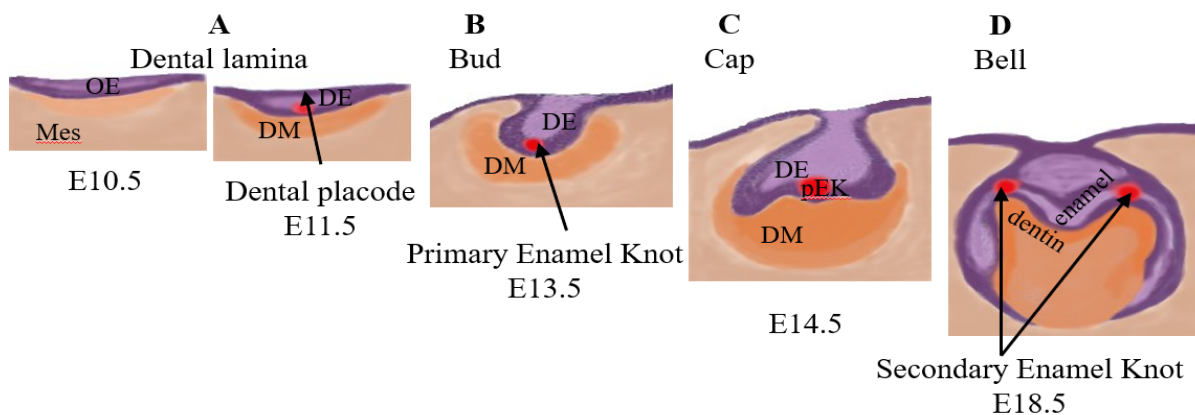


Figure 1. The four distinct stages of odontogenesis: (A) dental lamina formation at E10.5 and dental placode formation at E11.5, (B) bud stage at E13.5, (C) cap stage at E14.5, and (D) bell stage at E18.5. Dental epithelium (DE) and oral epithelium (OE) is shown in purple, condense underlying neural crest-derived mesenchyme (DE) is in dark orange, while rest of the mesenchyme cells (Mes) around the tooth formation area is shown in light orange. Signaling centers (i.e., dental placode at E11.5; primary enamel knot at (pEK) E13.5 & 14.5 and secondary enamel knot at E18.5) active at each stage are shown as red dots.

1.3 The integral role of *TP63* in initiating odontogenesis

One of the major transcription factors that required for epithelial cell layer development during odontogenesis is tumor protein 63 (*TP63*) (Yang et al. 2002; Belyi and Levine 2009; Joerggr et al. 2009). To date, it is commonly accepted that, compared to its homologues *TP53* and *TP73*, *TP63* most resembles the ancestral gene of the *TP53* family (Belyi and Levine 2009; Joerggr et al. 2009) and gene duplication events gave rise to the two additional homologs, *TP53*

and *TP73* (Belyi et al. 2010). The main function of the *TP53* family of genes is to protect the germline from DNA damage. In response to DNA damage caused by mutations, these proteins prevent the gene repair process and initiate apoptosis so that the mutation is not passed on in the germ-line (Belyi et al. 2010).

The *TP63* gene has two variants, one that contains an N-terminal transactivation domain (*TA-p63*), and another that does not (*ΔN-p63*) (Yang et al. 1998). Each of the two variants gives rise to three different isoforms: alpha (α), beta (β), and gamma (γ), due to alternative splicing at the variants' C terminus (Yang et al. 1998; Mills et al. 1999). *TP63* is required to initiate and regulate the development of epithelial cell layers regardless of their ectodermal or endodermal origin (Koster et al. 2004; Yoh and Prywes 2015; Kouwenhoven et al. 2015). Targeted disruption of *TP63* (e.g., the Brdm2 mouse mutant generated by Mills et al. in 1999 (Fig. 2)) causes limb and skin defects, among other pathological phenotypes. This Brdm2 mouse model was valuable because it revealed the main functions of *TP63* in the proliferation and differentiation of epithelial cells (Mills et al. 1999). Studies using this *TP63* mutant showed that *TA-p63* isoforms are expressed in epithelial cells prior to *ΔN-p63* isoforms during embryogenesis. Also, these studies revealed that *TA-p63* isoforms are counterbalanced by *ΔN-p63* isoforms. This counterbalance means that *TA-p63* isoforms' expression shifts to *ΔN-p63* isoforms' expression to allow epithelial cells to respond to signals required for their maturation. Signals such as *Bmp4* and *Fgfs* that come from underlying neural crest-derived mesenchymal cells (Yang et al. 1999; Mills et al. 1999; Koster et al. 2004). Further studies revealed, odontogenesis relies on activity of *ΔN-p63* isoforms (Rufini et al. 2006). During epithelial and tooth development *TP63* alpha and beta isoforms but not gamma isoform are predominantly expressed (Laurikkala et al. 2006). Also, other studies on this mutant showed that *TP63* regulates epithelial cell adhesion, integrity,

and homeostasis. In particular, *TP63* mediation of extracellular matrix adhesion molecules plays a critical role in normal epithelial-mesenchymal interactions (Carroll et al. 2007).

In *Brdm2* mutant mice, in which both *TP63* alleles are mutated (*TP63*^{-/-}), all epithelial derivatives are malformed if they are not actually missing (Fig. 2A) (Mills et al. 1999). This severe *TP63*^{-/-} phenotype indicates that *TP63* is crucial during the development of structures with epithelial origin such as limbs, skin, hair follicles, and teeth (Laurikkala et al. 2006), that also all require uninterrupted epithelial-mesenchymal crosstalk (Yang et al. 1999; Kouwenhoven et al. 2015). However, while the *TP63*-null mutant fails to form teeth because odontogenesis arrests shortly after it begins, the lower jaw (mandible) develops normally (Fig. 2D) (Paradis et al. 2013). It is salient to note that the mammalian mandible is composed of only the dentary bone, which has an exclusively mesenchymal origin. Therefore, *TP63* has an integral role in initiating odontogenesis and dental epithelium proliferation and differentiation that is exclusive of mandible morphogenesis (Rufini et al. 2006; Matsuura et al. 2012; Raj and Boughner 2016).

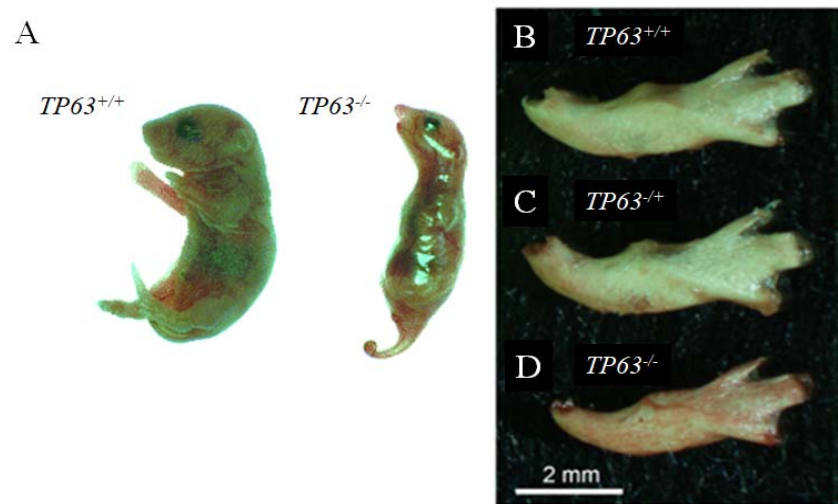


Figure 2. (A) Neonatal *Brdm2* mouse (right) showing the two *TP63* mutated alleles (*TP63*^{-/-}) phenotype that lacks epithelial derivatives, in comparison to neonatal wild-type mouse (left, *TP63*^{+/+}) (Adapted from Mills et al. 1999). (B-D) Comparing mandible (dentary bone) shapes among (B) *TP63* wild-type (*TP63*^{+/+}), (C) *TP63* heterozygote (*TP63*^{+/-}) and (D) *TP63*-null fetuses (E18) (*TP63*^{-/-}) shows that the dentary bone develops normally but with a 12-24 hours developmental delay in the toothless mouse (Adapted from Paradis et al. 2013).

1.4 Thesis research questions and objectives

1.4.1 Adding new genes to a *TP63*-mediated gene regulatory network active during mouse embryonic development

In *TP63*^{-/-} mice, tooth development arrests at E11.5, shortly after odontogenesis has initiated; consequently, no tooth buds ever form ([Laurikkala et al. 2006](#)). To better understand the genes that regulate odontogenesis exclusive of jaw development, a recent publication by [Raj and Boughner \(2016\)](#) used high-throughput gene expression microarray assays validated by reverse-transcription quantitative PCR (RT-QPCR) to contrast gene transcripts between the RNA extracted from surgically excised mandibular prominences in toothless *TP63*^{-/-} and toothed wild-type mouse embryos. This microarray screen identified a set of genes with significantly increased or decreased levels of expression in *TP63*-null mice compared to wild-type littermates at embryonic days (E) 10-13, four ages that encompass the earliest stages of tooth formation (Table 1). Among this set of genes, some had never before been connected to odontogenesis or to the *TP63* pathway. To more precisely understand the roles of these newly flagged genes in odontogenesis, the exact expression domains of these genes during the early stages of tooth development needed to be probed. Also, to connect these genes to a *TP63*-mediated gene regulatory network (GRN), changes in the expression of these genes relative to functional *TP63* presence or absence needed to be studied. In [Raj and Boughner's \(2016\)](#) study, several genes had significantly different fold changes between mutant and toothed strains that were either increased (positive fold changes) or decreased (negative fold changes). Also, comparison of the fold changes among different stages (E10-13) showed the changes in some of these genes were not only limited to one stage, but were consistent across all the stages (E10-13). The genes with the largest differences in expression levels (highest/lowest fold changes) which had not been previously connected to the odontogenesis were the ideal candidates for this thesis research.

Table 1. Results of microarray analysis showing the differences in gene expression caused by the null mutation of TP63 during odontogenesis. Fold changes of the genes that I studied here are: *Fermt1* (-2.9, -2.1), *Pltp* (-2.2, -1.6), *Cbln1* (2.2,2.3), and *Krt8* (2.7,4.5) at early stages of tooth development (E11,13). These genes showed constant decrease (*Fermt1* and *Pltp*) or increase (*Cbln1* and *Krt8*) in their fold changes. For example: *Fermt1* has significant fold changes (lower expression in *TP63*^{-/-} in comparison to wild type) in both E11 and E13. (Adapted from Raj & Boughner 2016).

Gene	Fold Change				Gene associated with:	
	E10	E11	E12	E13	odontogenesis	p63
<i>TP63</i>	-2.7	-2.1	-1.9	-2	Laurikkala et al., 2006	Mills et al., 1999
<i>Fermt1</i>	-2.7	-2.9	-2.3	-2.1	-	-
<i>Pltp</i>	-2.3	-2.2	-1.8	-1.6	-	-
<i>Cbln1</i>	1.8	2.2	2.6	2.3	-	-
<i>Krt8</i>	2.4	2.7	4.1	4.5	-	De Rosa et al., 2009

Therefore, my aim in this project was to add and connect four of these genes, Fermitin1 (*Fermt1*), Phospholipid Transfer Protein (*Pltp*), Cerebellin-1 (*Cbln1*), and Keratin 8 (*Krt8*), to a novel *TP63*-controlled GRN that is specific to odontogenesis but that does not influence jaw development. In the next section I briefly explain the known roles of these four genes.

Fermt1 is one of the Fermitin family homologues and is also known as *Kindlin 1*. This gene family encodes a group of highly conserved proteins called Fermitins. All the members of this family contain a FERM domain, the name coming from the first proteins that identified in this family: Four-point-one, Ezrin, Radixin, and Moesin (Pearson et al. 2000). Fermitins mediate the integrin activation and initiation intracellular signals called integrin inside-out signaling (Malinin et al. 2010). The gene *Fermt1* generally expresses in epithelium and encodes a cell structural protein linking actin to the extracellular matrix (ECM) (Jobard et al. 2003; Siegel et al. 2003). Next, Phospholipid Transfer Protein (*Pltp*) gene encodes the PLTP protein along with three other proteins that are all members of the lipid transfer/lipopolysaccharide binding protein (LT/LBP) gene family (Albers et al. 1996). The main established role for PLTP is the metabolism of lipoproteins. The PLTP protein also has the ability to bind to lipids and transfer

lipids between plasma lipoproteins t(Lagroste et al. 1998). Third, Cerebellin-1 (*Cbln1*) encodes CBLN1 which is a secreted glycoprotein. This protein is critical for synaptic integrity and function in neurons of brain cerebellar granule (Hirai et al. 2005). CBLN1 belongs to a protein family (CBLN1-CBLN4) which all share the C1q domain at their C termini (Urade et al. 1991). Lastly, Keratin 8 (*Krt8*) encodes KRT8, one of the many Keratin proteins. These proteins are the major component of intermediate filament proteins and predominantly expressed in epithelial cells (Makino et al. 2009). Keratin proteins are divided into two types based on their molecular weights: type I (K9-22), and type II (KRT1–KRT8) (Hesse et al. 2001). KRTs are essential cytoskeletal components important for cell morphology, mitosis, differentiation, and apoptosis (Tan et al. 2017). KRT8 expresses in tumors and has been associated with tumor progressions, notably cell migration, adhesion, and drug resistance (Fang et al. 2017).

1.4.2 Mapping the expression of four new genes at the beginning of tooth initiation and at the later bud stage of tooth development

In summary, none of these four genes had previously been linked to tooth development and despite the results of the microarray screen, it is not known exactly where in the developing tooth each gene may be expressed. Here I hypothesized that in normal dental epithelial cells, *TP63* up-regulates *Fermt1* and *Pltp*, and down-regulates *Cbln1* and *Krt8*. To test this hypothesis, I used *digoxigenin-labeled* RNA probe *in situ* hybridization to localize and map the expression of these four genes in dental and oral epithelium, as well as in underlying mesenchyme, and compare the expression of these genes in *TP63*-null mice with wild-type littermates. The expression domain and intensity of these genes were studied at two different time points of tooth development: E13.5, when the tooth bud formed in WT, and E11.5, when dental placode is fully form and starts signaling. Both of these stages overlap with two of the four stages studied by Raj and Boughner's (2016) microarray work.

CHAPTER 2 - MATERIALS AND METHODS

2.1 Study methodology: Overview

My data were collected from RNA *in situ* hybridization (ISH) experiments performed on sections of paraffin-embedded embryonic mouse heads. Mice were phenotyped and genotyped to identify Brdm2 toothless mutants (*TP63*^{-/-}) and toothed wild-type (*TP63*^{+/+}) embryos. Next, wild-type and mutant mice aged embryonic day (*E*) E13.5 and E11.5 were collected for RNA ISH. Embryos were fixed in paraformaldehyde (PFA), dehydrated in graded ethanol washes, embedded in paraffin, then sectioned and slide-mounted. I probed these tissue sections for four genes: *Fermt1*, *Pltp*, *Cbhl1*, and *Krt8*. As positive controls, I used Sonic Hedgehog (*Shh*) for both toothless and toothed mice, since *Shh* is expressed in dental epithelium where future teeth will form (Koyama et al. 1996). I used *TP63* as another positive control for toothed mice since, similar to *Shh*, *TP63* expresses intensely in oral and dental epithelium but is missing in the toothless mice. Sense RNA probes were used as negative controls. Both anti-Sense and Sense RNA probes were designed and synthesized by me. At least two different embryonic specimens were assayed per gene, for each time point.

2.2 Study materials

2.2.1 Mice

All the following studies were performed using pregnant and prenatal mice derived from the B6.129S7-*TP63tm2Brd/J* strain (Jackson Laboratory, Bar Harbor, U.S.A.) and *C57BL/6J* (stock # 003568 and # 000664, respectively). All mice were cared for by animal technicians in the Vivarium in the Health Sciences Building at the University of Saskatchewan. This care included breeding heterozygote adult mice and watching for vaginal plugs, which indicate

pregnant females. After 11 or 13 days post-coitum, pregnant dams were sacrificed by cervical dislocation in accordance with University of Saskatchewan animal use protocol # 20110008. Immediately after sacrifice, dissection forceps were used to extract all embryos from the uterus, which was immersed in 10X Phosphate Buffered Saline (PBS, Molecular Biology grade), under a dissecting microscope (Olympus, model SZX2ILLK).

2.2.2 Phenotyping

Brdm2 toothless mutants ($TP63^{-/-}$) were clearly distinguished from phenotypically normal wild-type ($TP63^{+/+}$) and heterozygote ($TP63^{+/-}$) embryos. From at least E9.5, homozygote mice have conspicuous morphological deformities, most notably their highly atrophied or absent limb buds (Mills *et al.* 1999). As such, these $TP63^{-/-}$ embryos did not need to be genotyped; however, homozygote tail clips were collected and used as positive controls for the polymerase chain reaction (PCR) work. In contrast, because heterozygote and wild-type mice are morphologically indistinguishable from each other, PCR was performed on these embryonic tissues using primers complementary to the $TP63$ insertion mutation (Jackson Laboratory, Bar Harbor, U.S.A.) (Table 2).

2.3 DNA extraction and genotyping

Each embryonic tail clip was collected in its own sterile (DNase/RNase-free) microcentrifuge tube and immediately snap-frozen dry at -20° Celcius (C) for subsequent DNA extraction and PCR work. All DNA extraction was done using a Phire Tissue Direct PCR master mix (Thermo Scientific, Waltham, U.S.A.). First, DNA release buffer (0.5 μ l) and dilution buffer (20 μ l) were added to each tissue sample, and then incubated at room temperature (RT) for 5 min. Next, samples were heated at 98° C for 2 min. After this step, the supernatant was collected and used immediately for PCR work or stored at -20° C until the next day, when the samples were

thawed, and used for PCR work. Extracted DNA was tested for quantity and quality using a NanoDrop Lite Spectrophotometer (Thermo Scientific). PCR was performed using the primers listed in Table 2. The presence of the *TP63* insertion mutation was detected with its specific primers (Table 2, top two rows). If the insertion mutation was present in the DNA sample, these primers amplified an insertion mutation that yields a sequence that is 410 base pairs (bp) in length. As an internal positive control, the genomic sequence coding for *T cell receptor* was amplified, with a product length of 210 bp (Table 2). A wild-type embryo would show a band for only this 210 bp band.

Table 2. List of PCR primers that were designed and validated by Jackson Laboratories and purchased from Sigma. Please refer to the following link for more primer and *PCR* protocol information:

http://jaxmice.jax.org/protocolsdb/f?p=116:2:753578398088607::NO:2:P2_MASTE_R_PROTOCOL_ID,P2_JRS_CODE:5248,003568.

<i>TP63</i> Insertion mutation	Forward (oIMR1029) 5' GTGTTGGCAAGGATTCTGAGACC 3'
	Reverse (oIMR1030) 5' GGAAGACAATAGCAGGCATGCTG 3'
<i>T cell receptor</i>	Forward (oIMR8744) 5' CAAATGTTGCTTGTCTGGTG 3'
	Reverse (oIMR8745) 5' GTCAGTCGAGTGCACAGTTT 3'

All PCR reaction ingredients listed below were stored at -20°C and thawed on ice before they were mixed to prepare the master reaction mixture (Table 3).

Table 3. Each PCR reaction mixture consisted of the following reagents:

Ingredient	Volume (μl)
Forward Primer (20 μM)	0.375
Reverse Primer (20 μM)	0.375
10x Buffer - MgCl ₂ (Invitrogen)	1.5
dNTP 10 μM (Invitrogen)	3.0
50x MgCl ₂ (Invitrogen)	0.75
Ultra pure H ₂ O (Gibco)	7.85
DNA (100-200 ng)	0.5-1.0
Total volume	14.35-14.85

After heating the thermocycler (Bio-Rad, Hercules, U.S.A.) to the temperature noted in Step 1, Table 4, the program was paused. While the sample tubes were still on ice, 0.150 μl of *TAQ* polymerase (Taq DNA Polymerase, recombinant CAT# 10342020,500 *units*) was added to each reaction mixture. Then all of the tubes were placed into the thermocycler, and the program was resumed and allowed to run to completion.

Table 4. Thermocycler program:

Step 1. 94°C for 5min
Step 2. 94°C for 30sec
Step 3. 55°C for 30sec
Step 4. 72°C for 30sec
Step 5. Back to step 2 and repeat 32x
Step 6. 72°C for 5min
Step 7. 4°C hold

Once the PCR was finished, all the tubes were removed from the thermocycler and placed on ice. Next, 2µl of 5x *BlueJuice* gel loading buffer (Life Technologies, Carlsbad, U.S.A.) was added to each tube of PCR product, which was then loaded into a 1.5% agarose gel (Invitrogen UltraPure Agarose, Life Technologies, Carlsbad, U.S.A.). The electrophoresis gel was made in 1x TAE (2M tris acetate, 0.05M EDTA, pH 8.3. Life Technologies) with 4µl *GelRed* Nucleic Acid added (Gel Stain, 10,000x in water, Biotium, U.S.A.). The gel was then run for approximately 40 minutes at 120 Volts. Next, the gel was imaged using a *UVP* BioDoc-It imaging system (UVP, Upland, CA, U.S.A.), and photographed with *UVP*-software (VisionWorksLS) (Fig. 3).

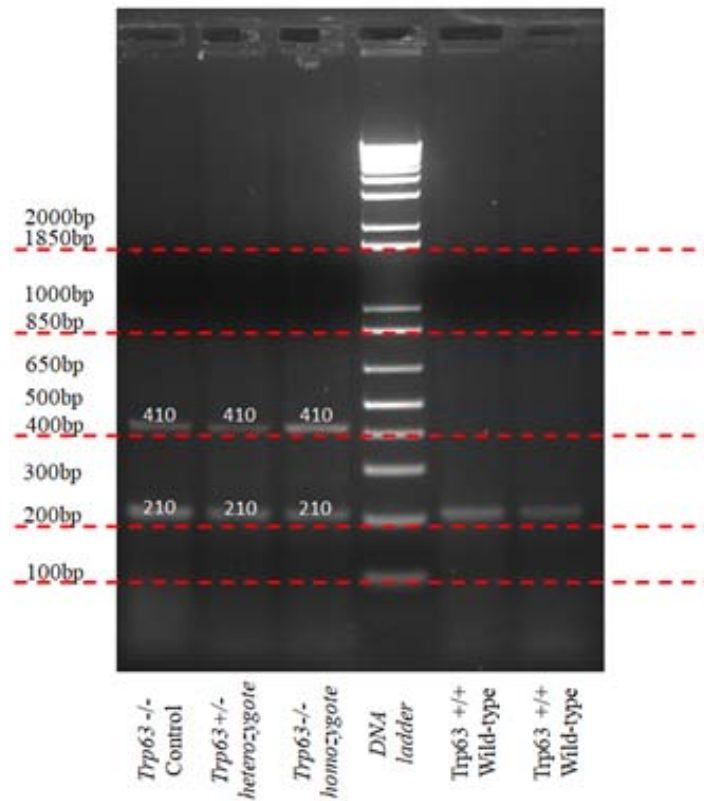


Figure 3. UV light view of a typical PCR agarose gel. Showing internal control band (210 bp) and mutated allele in $TP63^{-/+}$ (heterozygote) or $TP63^{-/-}$ (homozygote) via amplification of a 410 bp band. The absence of a 410 bp band indicates that both alleles are normal, and that the embryo is $TP63^{+/+}$ (wild-type), as shown below the gel image.

2.4 Embryo processing and sectioning

To perform the RNA probe *in situ* hybridization on paraffin tissue sections, first, dissected embryos were fixed overnight in 4% paraformaldehyde (PFA). (Note: fixative volume should be 20 times that of tissue on a weight per volume ratio; therefore, the whole embryo was immersed in 2 ml of 4% PFA.) The next day, tissues were washed twice in 1X PBS (in DEPC water) for 10 min at RT. Then, tissues were dehydrated with graded ethanol washes based on the following Table 5. After step 3, tissues were stored in fresh 70% EtOH/1X PBS at 4°C.

Table 5. Tissue dehydration steps. Ethanol washes used to dehydrate embryo samples.

Step 1. 1X wash in 25% EtOH/1X PBS for 15min at RT
Step 2. 1X wash in 50% EtOH/1X PBS for 15min at RT
Step 3. 1X wash in 70% EtOH/1X PBS for 15min at RT

Tissues were then processed through additional and graded washes of ethanol and xylene using a RVG/1 Vacuum Tissue Processor machine (Belair Instrument Company) located in the Core Histology Lab (Department of Anatomy & Cell Biology). Table 6 lists the processing protocol. Next, using a Tissue-Tek TEC 5 Tissue Embedding Console System (Model # 5100) processed tissues were embedded in paraffin blocks with heads in the coronal orientation. (See Table 6, following page.)

Table 6. Tissue processor progeam. Solutions and wash times used to process embryos:

Solution	Time	Temperature
EtOH 70%	1 hour	RT
EtOH 80%	1 hour	RT
EtOH 95%	35 minutes	RT
EtOH 95%	35 minutes	RT
EtOH 100%	50 minutes	RT
EtOH 100%	35 minutes	RT
EtOH 100%	35 minutes	RT
Xylene - 100% EtOH	45 minutes	RT
Xylene	40 minutes	RT
Xylene	40 minutes	RT
Paraffin	1hour	60°C
Paraffin	35 minutes	60°C
Paraffin	35 minutes	60°C
Paraffin	35 minutes	60°C

Once the paraffin blocks were allowed to solidify (overnight, at 4°C), each block was placed in a rotary microtome and oriented so that the blade cut straight across the paraffin block. Sections were cut at 8 µm thickness. Section thickness is important: sections must be thin enough for the probe to penetrate and thick enough to have enough tissue to detect RNA expression of the gene. Sections were picked up using tissue forceps and floated on a bath of 40-45°C DEPC-treated water in an autoclaved glass trough. After the sections were allowed to flatten out on the warm water, they were picked out of the water using Superfrost Plus microscope slides (U.S.A of Swiss Glass, CAT#12-550-15), placed on a slide warmer set at 37°C and left to bake overnight.

2.5 Hematoxylin and Eosin staining

Solutions:

Modified Harris Hematoxylin was used because it requires a less toxic chemical (sodium iodate instead of mercuric oxide), and the solution preparation is simpler and faster (no boiling of the solution is required). Staining results are comparable to the original solution.

Modified Harris Hematoxylin Working Solution:

100 g	Aluminum Potassium Sulfate ($\text{Al K}(\text{SO}_4)_2 \cdot 12\text{H}_2\text{O}$) Or Aluminum Ammonium Sulfate ($\text{Al NH}_4(\text{SO}_4)_2 \cdot 12\text{H}_2\text{O}$)
1000 mL	Distilled Water
5 g	Hematoxylin (<i>C.I. No. 75290</i>)
50 mL	Absolute Alcohol (i.e. 100% Ethanol)
0.5 g	Sodium Iodate
30 mL	Glacial Acetic Acid
Eosin Stock Solution: 1.25% Eosin Y (<i>C.I. No. 45380</i>) in 70% Ethanol (Add 1 mL of Glacial Acetic Acid to every 100 mL).	
Eosin Working Solution: 1-part Stock Solution to 4 parts 70% Ethanol	

Table 7. H & E staining protocol

3 minutes each	2 changes of Xylene
1 minute	Xylene / Absolute Alcohol
1 minute each	2 changes of Absolute Alcohol
1 minute	95 % Ethanol
1 minute	Tap Water
Rinse	Distilled Water
3 - 5 minutes	Harris Hematoxylin
Wash	Tap Water (several changes)
2 dips	Acid Alcohol (0.5% HCl in 95% Ethanol)
Wash	Tap Water (several changes)
5 seconds	Saturated Aqueous Lithium Carbonate
3 minutes	Running Tap Water
Rinse	Distilled Water
1 minute	Eosin
1 minute	95 % Ethanol
1 minute	Absolute Alcohol 1
1 minute	Absolute Alcohol 2
1 minute	Absolute Alcohol / Xylene
1 minute each	3 changes of Xylene
Leave slides in xylene until ready to coverslip; don't let them dry out! Coverslip (LOT#17907) slides in a permanent mounting medium.	

2.6 RNA *in situ* hybridization

I designed each RNA probe sequence based on that gene's cDNA sequence and sent these sequences to Bio Basic Company (Ontario, Canada) to be cloned. Then I synthesized the *Digoxigenin-labeled* RNA probe from the DNA plasmid returned to me by the company.

2.6.1 Designing RNA probes

To design the RNA probe, based on published mouse cDNA sequences I chose a specific fragment of the 3' *UTR* region of each gene of interest specifically since these 3' regions are unique for each gene. The length of each chosen fragments was between 500-900 bases. Also, gene protein sequences were BLASTed with other genes in the same family to exclude homology domains (using the multiple sequence alignment software T-COFFEE: <http://tcoffee.crg.cat/>) and protein conserved domains (using NCBI Conserved Domains software: <https://www.ncbi.nlm.nih.gov/Structure/cdd/wrpsb.cgi>). The T3 and T7 promoters were added specifically to the beginning and end of the RNA probe sequence. The final designed probe sequences were sent to Bio Basic Company (Ontario, Canada) to be cloned and inserted into pUC57 plasmids. Specifically, pUC57 is 2710 bp in length and is a high expression vector that is regularly used as a cloning vector in *E. coli*. This vector contains a *bla* gene for ampicillin resistance. Bio Basic returned by mail the lyophilized plasmids that I then transformed. First, before opening the container, I centrifuged the lyophilized DNA, then added TE buffer (10 mM, PH 8.5) and dissolved the DNA in TE buffer.

To transfer the plasmid into the bacteria, the appropriate *E. coli* competent cells were used (NEB 5-alpha competent *E. coli*, High Efficiency, CAT# C2987H). 100 ng of original plasmid DNA were added into *E. coli* competent cells and the mixture was incubated on ice for 30 minutes. Then, the mixture was heated at 42°C for 30 seconds and then immediately incubated on ice for 5 minutes. 950 µl *SOC* media were added to the mixture and incubated at

37°C for 60 minutes. This yielded my bacterial stock. 2µl of the bacterial stock was incubated on LB agar plates at 37°C overnight. The next day, a single colony that was well separated from other colonies was collected and inoculated in LB medium with Ampicillin, the antibiotic against which my plasmids are resistant, for large scale culture. The next day, DNA from the large culture was purified using a QIAprep Spin Miniprep Kit (CAT# 27104).

2.6.2 Probe synthesis

Making linearized template

1. I used a restriction enzyme that cuts a single site at the 5' end of the cDNA insert and linearized the plasmid equivalent to 10µg of DNA.

2. Mix:

10µg DNA
5µg of 10x buffer
4µg of restriction enzyme

3. Add Ultrapure distilled water (CAT#10977015) to a final volume of 50µl.

4. Incubate at 37°C for 3 hrs to overnight.

5. Transfer 2µl of DNA to a new 25 µl tube, mix with 7µl DEPC water and 1-2µl of loading dye, and run a 0.8% gel to check whether the DNA is linearized. (Also, run 1µl of uncut mini prep DNA as a control.)

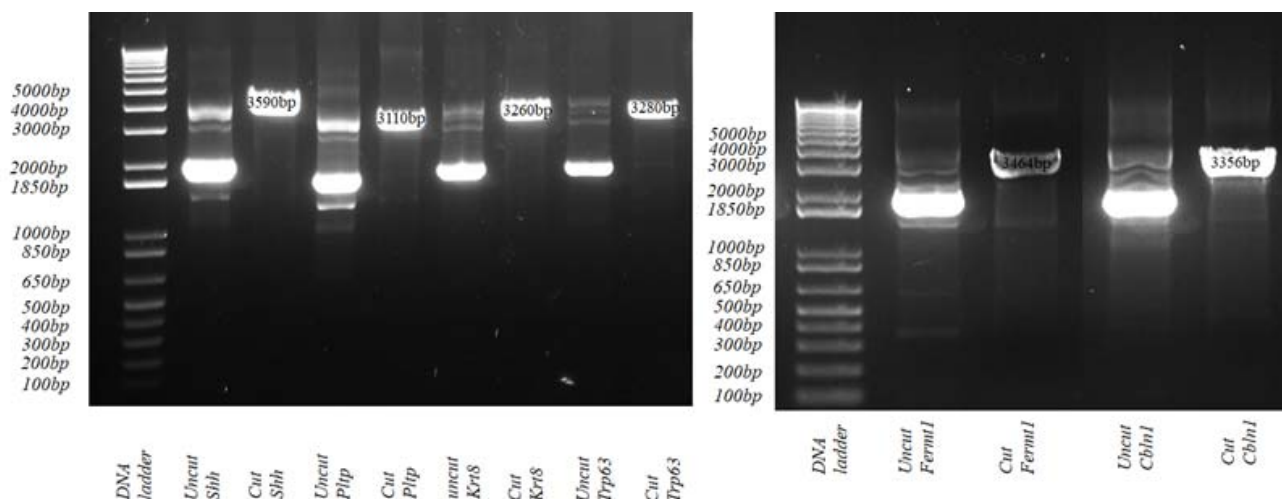


Figure 4. UV light view of agarose gel of all the genes of interest after DNA plasmids linearization, cut products along with their specific uncut stock DNA.

If the DNA wasn't cut properly then I repeated the linearization again.

If the DNA was cut properly then I proceeded to the following steps:

6. Add 100µl of ultrapure distilled water and 150µl of phenol/chloroform/IAA, mix, and spin at 10,000-15,000 rpm for 5min. Transfer only the top layer to a new tube.
7. Repeat step 6 (phenol/chloroform/IAA extraction).
8. Transfer the top layer to a new tube, extract with 150µl chloroform, and spin for 5 min.
9. Add 1/10 Vol of 3M sodium acetate and 2.5 volumes of ethanol, store at -70°C for 30 min.
10. Spin down at 10,000-15,000 rpm for 15 min at 4°C.
11. Carefully pipet off and discard the liquid. Wash the precipitate with 200µl of 80% ethanol, spin for 5 min, then pipet off and discard this liquid. Do a final quick spin and pipet with a sharp tip carefully to get rid of the last drops of EtOH.
12. Dissolve the precipitate in 40µl of ultrapure distilled water, and measure the concentration using a NanoDrop Lite Spectrophotometer (Thermo Scientific).

(Note: one could purify DNA using DNA clean up kit, instead of phenol/chloroform for purification. DNA clean up kit (for 5µg DNA): DNA clean and concentrator ZYMO CAT#D4003).

13. Transfer 1µl of the DNA to a new tube, mix with 7µl *DEPC* water and 1-2µl of loading dye, and run a gel to check whether you have gotten the DNA back.

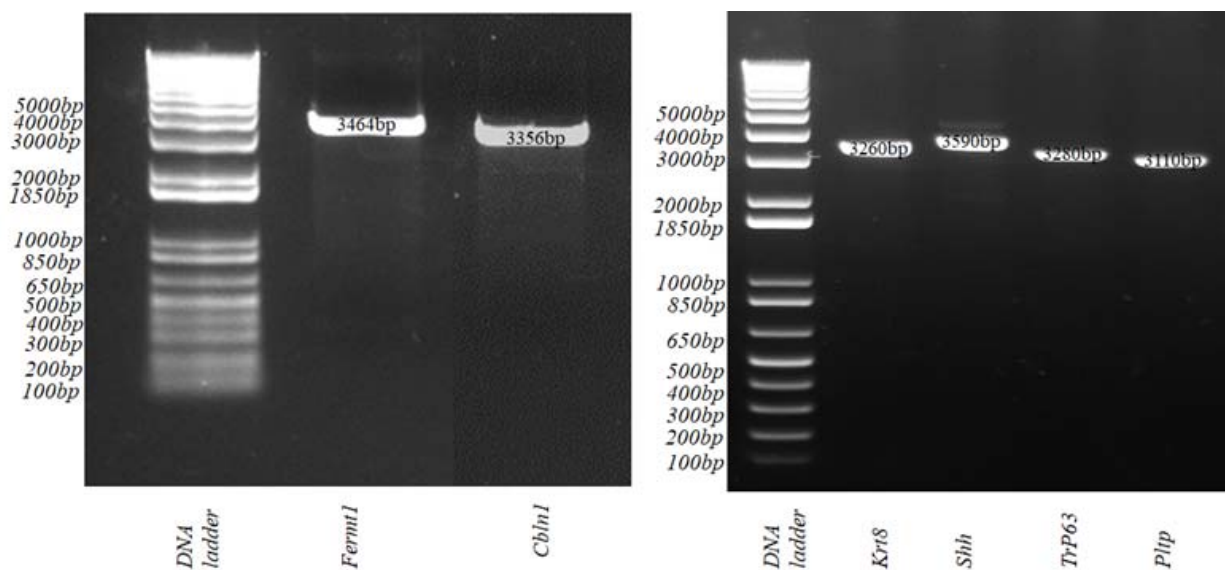


Figure 5. UV light view of an agarose gel showing all four of the genes of interest after DNA plasmid purification.

Making the RNA Probe

14. Mix together the 1X transcription reaction combine in a 1.5 ml tube:

1µg of linearized and purified plasmid (calculate volume based upon concentration)

2µl of 10X Transcription buffer (or 4µl of 5X buffer)

2µl of 10X nucleotide mix (with digoxigenin-UTP or fluorescein-UTP)

1µl of RNase inhibitor (40 units)

1µl of the appropriate T7, T3 (40u/µl) polymerase (20units/µl)

Ultrapure distilled water to give a final reaction volume of 20 µl

15. Incubate the mixture for 2hr at 37°C.

16. Add 4µl (40 units) of DNase 1 for 1X reaction. Incubate at 37°C for 15 min to remove the plasmid DNA.

17. Stop the reaction by adding 0.8 µl of 500mM EDTA pH 8.0.

18. Precipitate the RNA with 2.5 µl 4M LiCl, and 75 µl prechilled (-20°C) ethanol, keep at -70°C for 30min, if you can keep it longer you get better result.

19. Spin down the pellet at 10,000-15,000 rpm for 15min and discard the liquid.

20. Wash with 200µl of 80% EtOH then spin for 5min and discard the liquid. Next, do one quick spin for 10 seconds, and pipet with a sharp tip carefully to get rid of the last drop of ETOH.

(Note: one could use RNA clean up kit instead of ETOH precipitation. RNA cleans up kit: ZYMO CAT#R1015.)

21. Dissolve probe in 100 µl of RNase-free water containing (ultrapure distilled water) 1µl (40 units) of RNase inhibitor, and measure concentration using NanoDrop Lite Spectrophotometer (Thermo Scientific).

22. Check the probe's quality by running 2.5 µl of the stock volume on a 0.8% agarose, 1X TBE or TAE minigel. Wash the apparatus thoroughly before preparing the gel and run the samples quickly to avoid problems with RNase.

2.6.3 *in situ* hybridization

DAY 1

Deparaffinization:

1. Rehydration (in fume hood)

2x xylene, 5 minutes each

2x 100% EtOH, 1 minute each

1x 70% EtOH, 1 minute
1x 1X PBS, 5 minutes

2. Fix in 4% PFA-DEPC for 20 min.
3. Rinse 1X in 1X PBS for 5 min.
4. Incubate slides in 0.2N HCl-DEPC at RT for 10 min (use slide mailers).
5. Rinse 2X in 1X PBS-DEPC for 5 min each.
6. Proteinase K (3 µg/ml 1X PBS-DEPC) @37°C for approximately 10 -15 min.
7. Rinse 1X in 1X PBS -DEPC.
8. Post -fix in 4% PFA -DEPC for 15 min.
9. Pre -hybridize sections in hybridization buffer for 3 hours at 58°C.
10. Prepare the probe in 100 µl of hybridization solution at a final concentration of 0.2 -0.4 ng/µl. Heat at 70°C for 5 min, then put on ice. Load the probe onto the tissue sections and coverslip.
11. Incubate slides O/N at 58°C.

DAY 2

12. Transfer the slides to a slide Mailer immersed in washing solution (enough to cover the slides) at 58°C.
Wash 1X 15 min at 58°C to allow coverslips to fall off.
Wash 2X 30 min at 58°C in washing solution.
13. Wash 2X 30 min in 1X MABT.

Blocking and antibody staining:

14. Block at least 1 hour (2 -3 hours is desirable) in 1X MABT + 2% Blocking reagent + 20% heat inactivated sheep serum at RT (no coverslips).
15. Incubate O/N at 4°C with fresh 1X MABT + 2% Blocking reagent +20% sheep serum containing a 1 -1000 dilution of anti -DIG Alkaline Phosphatase antibody in a humidified chamber (with 1X PBS -DEPC). Use 100 µl per section and coverslip.

DAY 3

Post -antibody washes:

16. Transfer slides to a slide mailer immersed in 1X MABT (enough to cover the slides)
Wash 4x 30 min each in 1X MABT.

17. Wash 2X, 10 min each in AP staining buffer. Use a shaker at RT for this step.

Staining reaction:

18. Add 1ml per slide of BM purple AP substrate and keep the slides in humidifier chamber protected from light, for 1 -24 hours at RT to reveal the expression.

19. Wash 3X, 5 min each in PBS.

20. Dehydrate with EtOH:

Wash slides 1X for 5 min in 70% EtOH.

Wash slides 1X for 5 min in 95% EtOH.

Wash slides 2X, for 5 min each in 100% EtOH.

21. Mount slides in permount for photography.

SOLUTIONS (all solutions are prepared with DEPC water)

4% PFA in PBS - mix 4g paraformaldehyde (PFA) with 100ml 1X PBS.

Place on a heating block until solution becomes clear, immediately filter into a bottle placed on ice aliquot and freeze. Aliquots can only be thawed once

10X Salt - 2M NaCl, 100 mM Tris -HCl pH 7.5, 100mM phosphate buffer pH 7.4, 50 mM EDTA pH8
100 ml 5M NaCl 25 ml 1M Tris -HCl pH7.5 25 ml 0.5M EDTA 19.35 ml 1M Na₂HPO₄ 5.65 ml 1M NaH₂PO₄ H₂O QSP 250 ml

50X Denhardt's - 100 ml stored aliquoted at -20°C

1gm bovine serum albumin (1% W/V)

1gm FicollTM (1%W/V)

1gm polyvinylpyrrolidone (Mol.Wt. 360,000)

Make up to 100 ml with ddH₂O

Hybridization buffer - stored aliquots at -20°C

	10ml	20ml	50ml	100ml	Final Conc
1X salt	1ml	2ml	5ml	10ml	1X
Deionized formamide	5ml	10ml	25ml	50ml	50%
dextran sulphate	1gm	2gm	5gm	10gm	10%
Torula RNA 1 mg/ml	200µl	400µl	1ml	2ml	1mg/ml
50X Denhardt's	200µl	400µl	1ml	2ml	1X
ddH ₂ O	3.6ml	7.2ml	18ml	36ml	

Washing solution - 1X SSC, 50% formamide, 0.1% Tween20

1X MABT - 100 mM maleic acid, 150mM NaCl, 0.1% Tween20, pH 7.5

5X MAB - 21.91g NaCl 29.02g Maleic Acid pH to 7.5 with NaOH - first add 18g NaOH pellets, then adjust pH with concentrated NaOH solution H₂O QSP 500ml

Blocking reagent - Roche CAT# 11 096 176 001. Make 10% stocks in 1X MAB (no tween20) and store at -20°C

Alkaline phosphatase (AP) buffer

****Prepare freshly just before use from stock solutions.**

Stock Soln.	100ml	Final Conc.
5M NaCl	2 ml	100 mM
1M MgCl ₂	5 ml	50 mM
1M Tris pH 9.5	10 ml	100 mM
20% Tween 20	0.5 ml	0.1%
ddH ₂ O	82.5 ml	- - - - -

2.7 Gene expression documentation

Gene expression domain and intensity were visually mapped and analyzed based on the pattern of the BM purple dye location. To document the gene expression domains and intensities, slides of the assayed tissue sections were photographed using a digital camera (Olympus, model: DP21, D21-CU) and dissection microscope (Olympus, model SZX2ILLK).

CHAPTER 3 - RESULTS

Recent work by Raj and Boughner (2016) flagged a new set of the genes that showed significant increases or decreases in their expression levels in the mandibular prominences (MdPs) of *TP63*-null mice (*TP63*^{-/-}) compared to wild-type littermates at embryonic days (E) 10-13. In this MSc thesis project, I characterized the expression domain and intensity of four of these genes - *Fermt1*, *Pltp*, *Cbln1*, *Krt8* - in mouse tooth organ using Antisense *Digoxigenin-labeled* RNA probe *in situ* hybridization. I hypothesized that *TP63* up-regulates *Fermt1* and *Pltp*, and down-regulates *Cbln1* and *Krt8*, in dental epithelial cells.

3.1 Digoxigenin-labeled RNA probe synthesis results

In this project, all the RNA probes were designed by me and this was the first time that these probes were used in embryonic mouse dental and jaw tissues. Therefore, after my antisense and sense *Digoxigenin-labeled* RNA probes were synthesized, to confirm the size of the probes I ran all of them on a 0.8% agarose gel. Figures 6 and 7 show the UV light view of these agarose gels. RNA probes usually appear as a smear instead of a single band. I used a DNA ladder (CAT# 10787018) as a guide for the RNA probe sizes. Smears located at about the size that was expected for each probe is evidence that the probe was successfully synthesized (Fig. 6, 7). Also, as another check, probes were sent for sequencing to Eurofins Genomics company, and sequencing results were blasted against published sequences of mRNA. This confirmed that my antisense probes were the reverse complements to published mRNA sequences (Appendix A). In contrast, sense probes (my negative controls) were same sequences as for published mRNA.

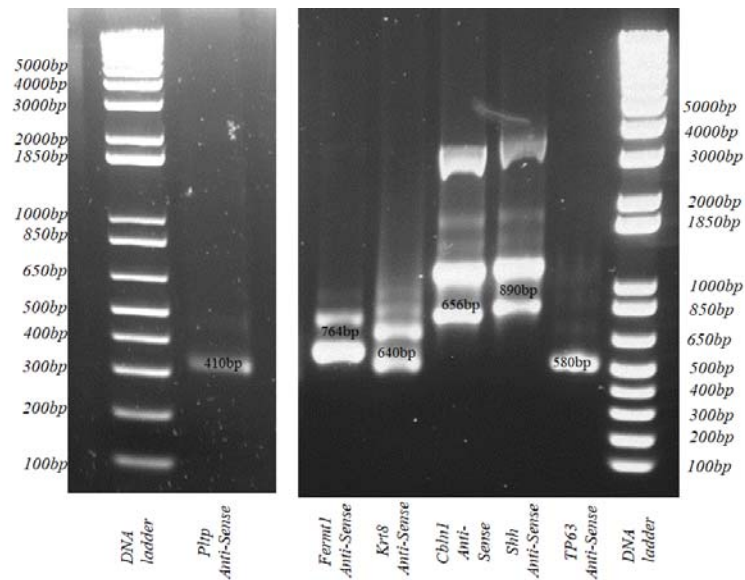


Figure 6. UV light view of an agarose gel showing antisense probes for six genes and smears approximately around the size that was expected.

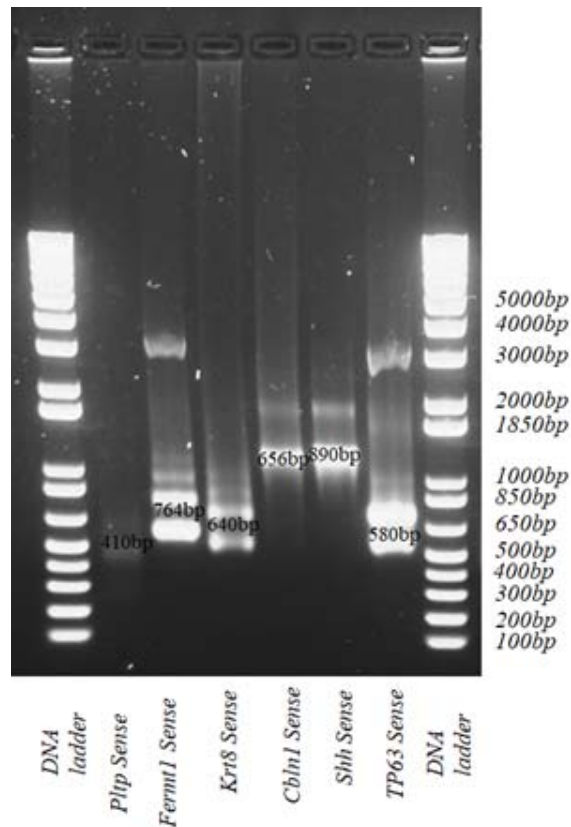


Figure 7. UV light view of an agarose gel showing sense probes for six genes and smears approximately around the size that was expected. The expected size for sense probe is same as antisense probe for the same gene.

In situ hybridization (ISH) assays probed coronal tissue sections of wild-type (*WT*) and *TP63*-null (*TP63*^{-/-}) embryos. Expression of *Fermt1*, *Pltp*, *Cbhl1* and *Krt8* were observed in the tooth organs of both the upper and lower jaw primordia. Two different stages of tooth development - placode and bud stages - were assayed to compare differences and changes in expression level of the same four genes, in addition to control genes *TP63* and *Shh*. The latter gene is a well-known marker for early tooth formation (Seppala et al. 2017). Embryonic day (E) 13.5 is the stage when the tooth bud forms in wild-type mice, and E11.5 is about the time when dental placode formation is arrested in the *TP63*-null mice. In this study, genes of interest and control genes ISH were performed on adjacent sections of each individual.

3.2 The expression of *TP63*, *Shh*, and four novel genes (*Fermt1*, *Pltp*, *Cbhl1*, and *Krt8*) in tooth organ and jaw at E13.5

I used H & E staining to help view and identify the tooth organ morphology (Fig. 8A). Hatched lines represent the dental epithelium in the tooth bud. My ISH results showed that, at bud stage, *TP63* expression in mice was restricted to oral and dental epithelium (Fig. 8B). *Shh* expression was restricted to the specific area of dental epithelium in both wild-type and *TP63*^{-/-} mice which were used as a marker to specify the dental epithelium in both models (Fig 9A-B, 10A-B). *Fermt1* expression in wild-type mouse was more intense in oral epithelium and dental epithelium than in dental mesenchyme (Fig. 9E). *Pltp* expression in the same wild-type individual was intense and more restricted to the dental epithelium than to the oral epithelium or dental mesenchyme (Fig. 9G). *TP63*, *Fermt1*, and *Pltp* expression domains in dental epithelium overlapped with each other in the wild-type embryos (Fig. 9A-C-E-G). Compared to their wild-type littermates, in the *TP63*^{-/-} mice *Fermt1* was expressed at very low intensity in the oral and dental epithelium (Fig 9F). In the same *TP63*^{-/-} mouse, *Pltp* expression was seen in the dental

epithelium but, compared to the littermate wild-type, the intensity of expression was decreased, notably in the dental epithelium (Fig. 9H). Decreased expression of *Fermt1* and *Pltp* in *TP63*^{-/-} embryos were mostly in the same area, which according to *Shh* expression was marked as dental epithelium (Fig. 9B-D-F-H). Conversely, *Cbln1* did not show any expression in the dental epithelium, oral epithelium, and dental mesenchyme in the wild-type mice (Fig. 10E), although *Cbln1* was expressed intensely in the dental epithelium of *TP63*^{-/-} littermates (Fig. 10F). *Krt8* expression was seen in both wild-type and *TP63*^{-/-} littermates and was restricted to the dental and oral epithelium in both mouse strains. Comparing *Krt8* expression intensity between wild-type and *TP63*^{-/-} littermates showed higher expression in *TP63*^{-/-} dental epithelium (Fig. 10G&H). Changes in the level of expression of *Cbln1* and *Krt8* in, are mostly in the same area that *Shh* expression flagged as the dental epithelium and that overlaps with differences in *TP63* expression.

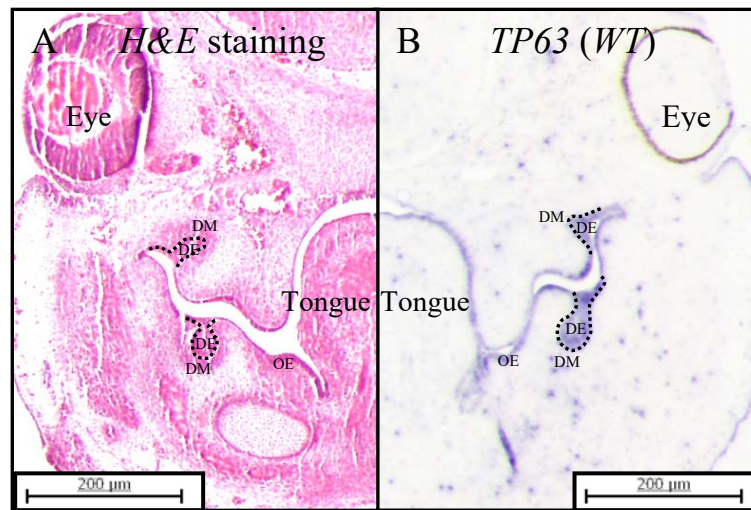


Figure 8. Coronal view of mouse head (A), showing tooth organ at bud stage (hatched lines are defining dental epithelium in tooth organ) and (B) *TP63* expression (purple) at E13.5 which is restricted to oral epithelium and dental organ. Oral Epithelium (OE), Dental Epithelium (DE), and Dental Mesenchyme (DM).

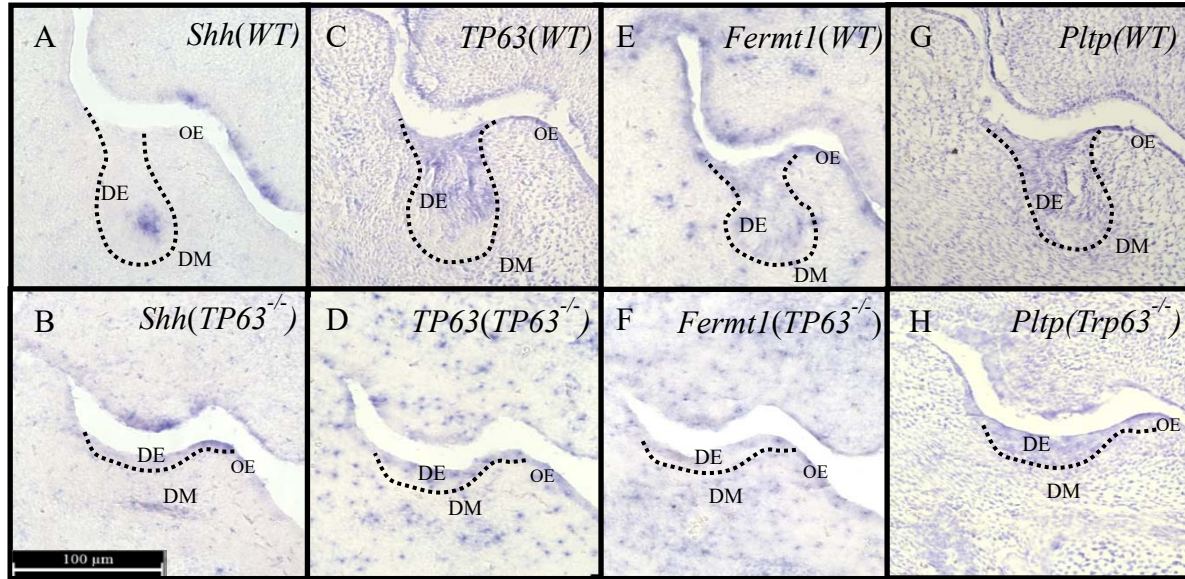


Figure 9. RNA *in situ* hybridization on coronal sections of tooth organ at E13.5 with expression of (A, B) *Shh* in dental placode used as positive controls in both *WT* (toothed) mice (top row) and *TP63*^{-/-} (toothless) mice (bottom row) and as guides to show where teeth normally form. Hatched lines are schematic representation of histology of tooth bud morphology and in *TP63*^{-/-} show the small thickening in oral epithelium, (C, D) Presence of *TP63* expression in dental epithelium and tooth organ in *WT* and absence of *TP63* expression in *TP63*^{-/-} mouse was confirmed, (E, F) expression level of *Fermt1* in dental epithelium in *WT* and *TP63*^{-/-} mice, (G, H) *Pltp* level of expression in dental epithelium in *WT* and *TP63*^{-/-} mice. *Fermt1* and *Pltp* express in dental epithelium and expression intensity for these two genes in *TP63*^{-/-} mice is lower than *WT*. Oral Epithelium (OE), Dental Epithelium (DE), and Dental Mesenchyme (DM)

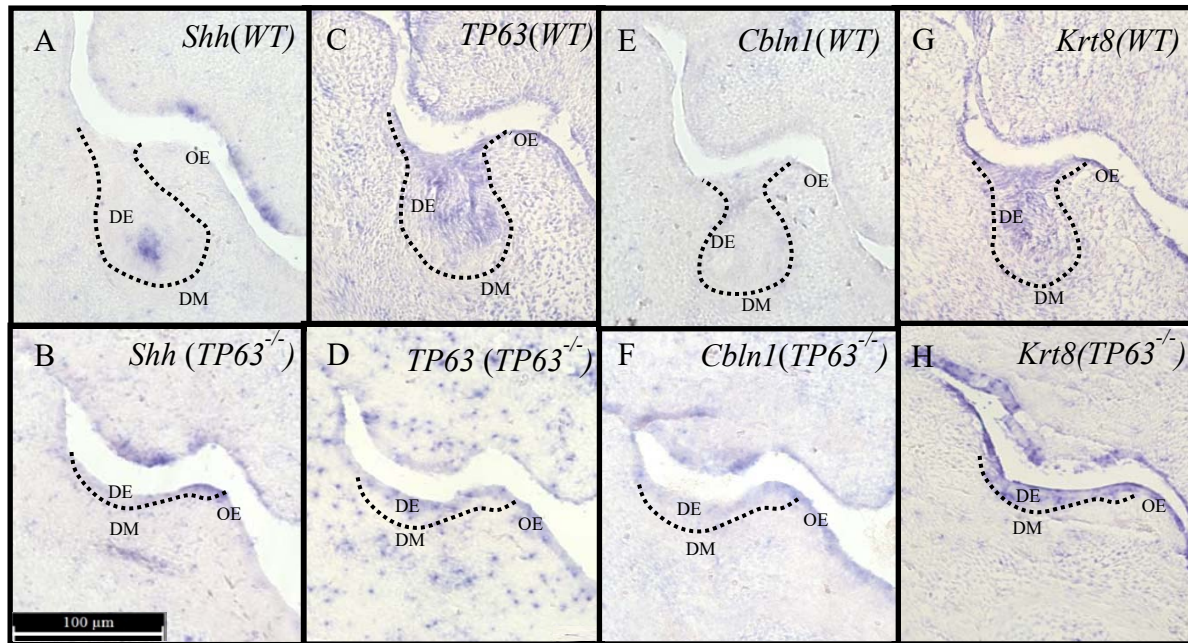


Figure 10. RNA *in situ* hybridization on coronal sections of tooth organ at E13.5 with expression of (A, B) *Shh* in dental placode that used as positive controls in both *WT* (toothed) mice (top row) and *TP63*^{-/-} (toothless) mice (bottom row) and as guides to show where teeth normally form. Hatched lines are schematic representation of histology of tooth bud morphology and in *TP63*^{-/-} show the small thickening in oral epithelium, (C, D) Presence of *TP63* expression in dental epithelium and tooth organ in *WT* and absence of *TP63* expression in *TP63*^{-/-} mice was confirmed, (E, F) *Cbhl1* level of expression in dental epithelium in *WT* and *TP63*^{-/-} mice, (G, H) expression level of *Krt8* in dental epithelium in *WT* and *TP63*^{-/-} mice. *Cbhl1* and *Krt8* express in dental epithelium and expression intensity of these two genes in *TP63*^{-/-} mice is higher than *WT*. Oral Epithelium (OE), Dental Epithelium (DE), and Dental Mesenchyme (DM).

3.3 The expression of *TP63*, *Shh*, and four novel genes (*Fermt1*, *Pltp*, *Cbln1*, and *Krt8*) in tooth organ and jaw at E11.5

After visually confirming the differences in expression level and domain of my four genes of interest at E13.5, I mapped the expression of these same four genes at E11.5. My *in situ* results at E11.5 align with my findings at E13.5, showing that these four genes expression domains are similar at early and later stages of tooth formation. Also, in the absence of functional *TP63*, *Fermt1* and *Pltp* expression decreased (Fig. 11), and *Cbln1* and *Krt8* expression increased (Fig. 12) in the dental epithelium at E11.5. These findings confirmed the previous microarray data regarding decrease and increase in the level of expression of these four genes at E11.5 and revealed that these changes happen in the same tooth organ domain as the later stage (E13.5).

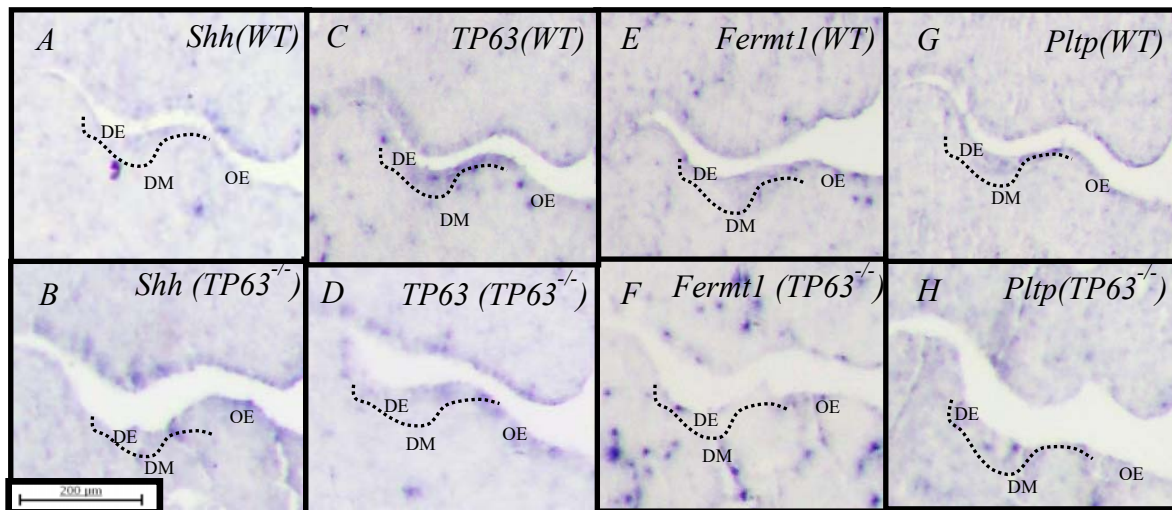


Figure 11. RNA *in situ* hybridization on coronal sections of tooth organ at E11.5 with expression of (A, B) *Shh* in dental placode that used as positive controls in both *WT* (toothed) mice (top row) and *TP63*^{-/-} (toothless) mice (bottom row) and as guides to show where teeth normally form. Hatched line showing typical dental epithelium thickening morphology, (C, D) Presence of *TP63* expression in dental epithelium and tooth organ in *WT* and absence of *TP63* expression in *TP63*^{-/-} mice was confirmed, (E, F) expression level of *Fermt1* in dental epithelium in *WT* and *TP63*^{-/-} mice, (G, H) *Pltp* level of expression in dental epithelium in *WT* and *TP63*^{-/-} mice. *Fermt1* and *Pltp* express in dental epithelium and expression intensity in *TP63*^{-/-} mice is lower than *WT*. Oral Epithelium (OE), Dental Epithelium (DE), and Dental Mesenchyme (DM).

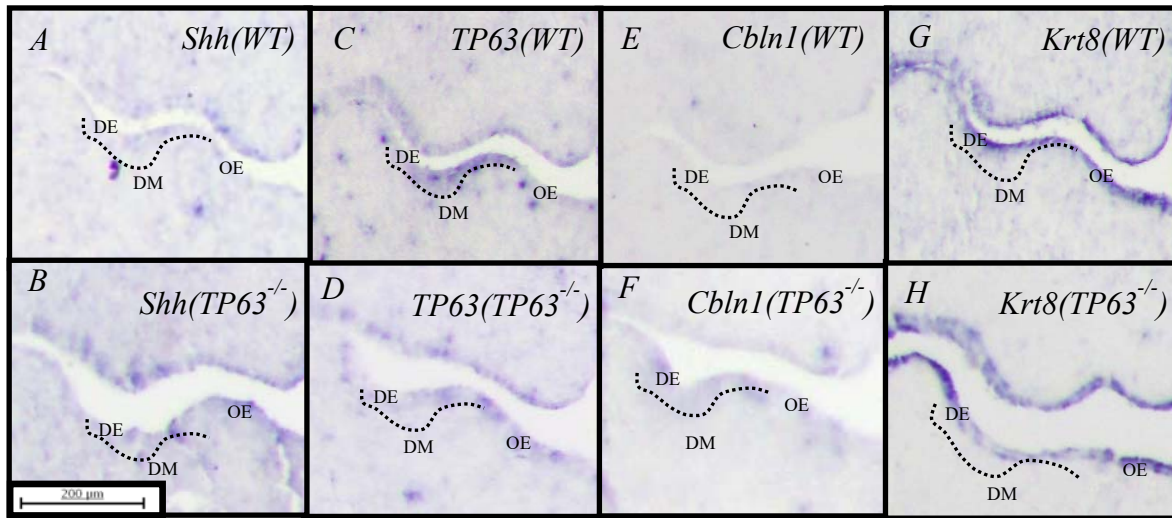


Figure 12. RNA *in situ* hybridization on coronal sections of tooth organ at E11.5 with expression of (A, B) *Shh* in dental placode that used as positive controls in both *WT* (toothed)mice (top row) and *TP63*^{-/-} (toothless) mice (bottom row) and as guides to show where teeth normally form. Hatched line showing typical dental epithelium morphology, (C, D) Presence of *TP63* expression in dental epithelium and tooth organ in *WT* and absence of *TP63* expression in *TP63*^{-/-} mice was confirmed, (E, F) *Cbhl1* level of expression in dental epithelium in *WT* and *TP63*^{-/-} mice. (G, H) expression level of *Krt8* in dental epithelium in *WT* and *TP63*^{-/-} mice. *Cbhl1* and *Krt8* express in dental epithelium and expression intensity in *TP63*^{-/-} mice is higher than *WT*. Oral Epithelium (OE), Dental Epithelium (DE), and Dental Mesenchyme (DM).

3.4 Negative controls using sense probes

Specific sense probes were used as a negative control for each specific gene, to confirm the accuracy of antisense probes expressions (Fig. 13).

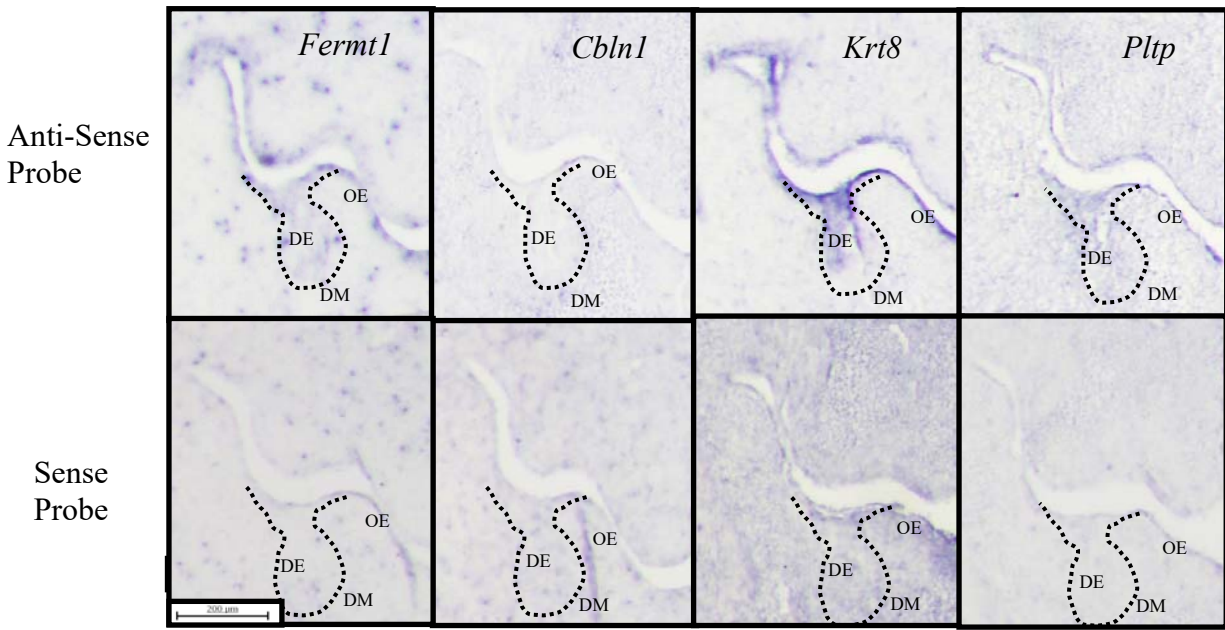


Figure 13. RNA *in situ* hybridization on coronal sections of tooth organ at E13.5, top row use of *antisense* RNA probes for *Fermt1*, *Pltp*, *Cbln1*, and *Krt 8* in *WT* mice, bottom row use of *sense* RNA probes for *Fermt1*, *Pltp*, *Cbln1*, and *Krt 8* in *WT* mice as a negative control for each probe. Oral Epithelium (OE), Dental Epithelium (DE), and Dental Mesenchyme (DM).

In summary, RNA *in situ* hybridization experiments revealed the expression domains of *Fermt1*, *Pltp*, *Cbln1*, and *Krt8* for the first time in mouse tooth organ. Also, these experiments visualized the correlation between the presence and absence of *TP63* with all four genes. Lastly, studying the expression domains and intensities of all four genes at two different time points during the earliest stages of odontogenesis suggested that each of these genes is targeted by *TP63* during early tooth formation. The expression of these four genes appears to be simultaneously affected by *TP63* expression.

CHAPTER 4 - DISCUSSION AND CONCLUSIONS

4.1 The importance of the *TP63* transcription factor and its gene regulatory network in the oral dentition in mammals

TP63 is one of the main transcription factors required for onset of odontogenesis (Laurikkala et al. 2006). My RNA *in situ* hybridization experiments using E11.5 and E13.5 aged *TP63*^{-/-} and wild-type mice visualized the expression domains of four genes of interest (*Fermt1*, *Pltp*, *Cbln1*, and *Krt8*) in the tooth organ. This thesis research also showed a strong correlation between the expression of *TP63* and that of the four other genes, *Fermt1*, *Pltp*, *Cbln1*, and *Krt8*, in embryonic tooth tissues. My work revealed that *Fermt1* and *Pltp* expression intensities decreased specifically in the dental epithelium in the absence of *TP63*. In contrast, *Cbln1* and *Krt8* expression intensities increased, also in the dental epithelium, in the absence of *TP63*. These results suggest that *TP63* up-regulates *Fermt1* and *Pltp*, and down-regulates *Cbln1* and *Krt8* in dental epithelial cells at early stages of tooth development.

Also, the expression domains and intensities of all four of these genes of interest in dental epithelium (which belongs to the first molar) are comparable between the lower and upper jaw primordia. This result is somewhat surprising because: 1) the molecular profiles that give rise to these two anatomically different facial structures differ (Lee et al. 2004), and; 2) even in the *TP63*^{-/-} mouse, the lower jaw forms normally while the upper jaw is typically deformed (Paradis et al. 2013), including presenting with midfacial clefting (Thomason et al. 2010). These results suggest that the role that *Fermt1*, *Pltp*, *Cbln1*, and *Krt8* play is important and equivalent during the early stage of tooth development in both the upper and lower dentitions. In *TP63*^{-/-} embryos the teeth but not jaws fail to form: comparing the level of expression of these four genes in dental

epithelium between toothed wild-type and toothless *TP63*^{-/-} embryos suggests that *Fermt1*, *Pltp*, *Cbln1*, and *Krt8* belong to a *TP63*-controlled gene regulatory network that drives odontogenesis with neither input from, nor influence on, jaw morphogenesis (Fig. 14).

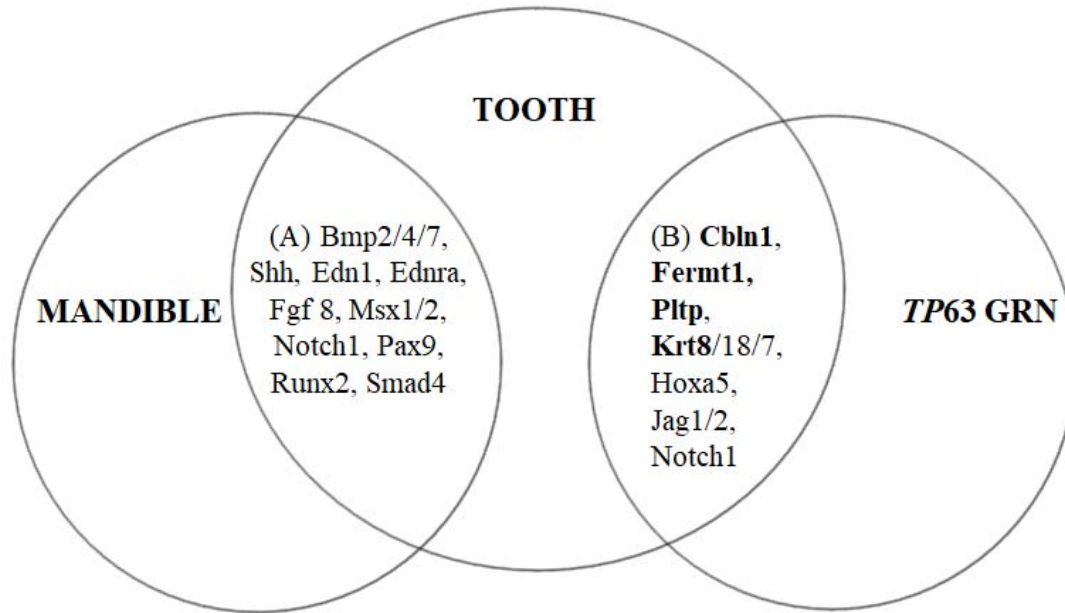


Figure 14. Venn diagram based on my recent ISH results, past microarray screens results and MGI/NCBI databases showing: **(A)** genes known to be important for mandible and tooth development that I posit do not act within a *TP63* odontogenic *GRN*; versus **(B)** candidate members of a *TP63* odontogenic *GRN* that have redundant/null roles for mandible morphogenesis. The four bold-font gene names (*Fermt1*, *Pltp*, *Cbln1*, and *Krt8*) are those genes presented here (Adapted from Raj & Boughner 2016).

These results also suggest that as early as E11.5 *TP63* plays a role in regulating the expression of all four genes of interest. E11.5 is an important stage of tooth development: first, the dental placode, which is the first signaling center, forms, and then regulates tooth bud formation. Second, in the *TP63*^{-/-} mouse, tooth formation is arrested, and the dental placode fails to form the tooth bud, due to absent *TP63* and perturbed signaling pathways that are important for tooth formation. Indirectly, my results suggest that four genes of interest are important if not indispensable to early tooth morphogenesis.

The *TP63* up-regulation effect on *Fermt1* and *Pltp*, and its down-regulation effect on *Cbln1* and *Krt8* in dental epithelium in two important time points of tooth formation suggests that each of these new genes (*Fermt1*, *Pltp*, *Cbln1*, and *Krt8*) that I connected to the dental epithelium, and to the *TP63* gene regulatory network more broadly, are distinct downstream targets of *TP63*. As next steps to build on my thesis work, protein expression profiling, study of later stages of tooth development, and functional study of these four genes are needed to understand how the expression of these genes might change relatively to each other and to help test the reliability of my hypothesis that the four genes play a key role in earliest odontogenesis. In the next section I focus on the putative roles that each of the four genes might play in the developing tooth.

4.2 Putative roles of these four new candidate genes in a tooth-specific *TP63* gene regulatory network

Fermt1 has been studied intensively, with a focus on its function in keratinocytes and skin. Herz et al., (2006) showed that FERMT1 protein is expressed in epidermal keratinocytes, which are located near the skin basement membrane. This study also revealed that, due to FERMT1 deficiency in skin cells, the proliferation of keratinocytes was significantly reduced. Also, *in vitro* experiments confirmed that *Fermt1* deficiency in cultured keratinocytes caused the same disease phenotype seen in human skin (Herz et al. 2006). This phenotype, called *Kindler* syndrome, is a rare autosomal recessive genodermatosis caused by a mutation in *Fermt1*. Fragile and blistering skin are the main characteristics of this syndrome (Has et al. 2011). Also, work on *Fermt1* deficiency in keratinocytes showed that this gene encodes a protein with an important role in cell adhesion to the extracellular matrix, cell migration, and proliferation (Herz et al. 2006). Based on previous studies of FERMT1, this protein seems necessary for keratinocyte

homeostasis, binds to and activates integrin, and is involved in epithelial cell adhesion to the extracellular matrix ([Calderwood et al. 2013](#)).

Although in some databases ([e.g., genecards.org](#)), *Fermt1* expression in dental epithelium has been reported, I couldn't find a specific publication that reported the results and the exact expression domains or role in tooth organ for this gene. The novel ISH results that I presented in this thesis define the wild-type expression domain of *Fermt1* in dental epithelium during early odontogenesis, both placode and bud stages, and show decreased *Fermt1* expression in the dental epithelium of same-aged *TP63*-null mice. Since this gene is required for epithelial cell adhesion to the extracellular matrix, cell migration, my results along with those from previous studies suggest that *Fermt1* helps normal dental epithelium cell shape and polarity. I also suggest that *Fermt1* helps to maintain the bond between dental epithelium cells and their extracellular matrix and, consequently, the underlying mesenchyme. This physical bond helps the epithelium and mesenchyme to signal to each other, which is vital for dental epithelium maturation and proliferation, as well as for mesenchymal cell proliferation at later stages.

Next, *Pltp* has primarily been studied relative to lipid metabolism ([Albers et al. 1995](#)). In general, the majority of published studies on PLTP function focus on how this protein relates to high-density lipoprotein (*HDL*) and low-density lipoprotein (*LDL*) metabolism, and suggest that PLTP has a key role in lipoprotein metabolism and lipid transport ([Albers et al. 2012](#)). PLTP is secreted by a variety of tissues. [2003, O'Brien et al.](#)'s study on human atherosclerosis (in which plaque accumulates inside arteries) suggested that PLTP accumulates on the extracellular matrix and acts as a connecting molecule to mediate the *HDL* binding to ECM. Many cellular processes during tooth development such as epithelium cells migration, proliferation, and differentiation affect cell adhesion to other cells and the ECM. Lipids in the epithelial cell membrane are crucial

for the maintenance of cell adhesion structures. These structures along with lipids in the cell membrane enable epithelial cells to attach to ECM (Márquez et al. 2008). Also Márquez et al. in 2012 revealed lipid composition in the epithelial cell membrane has a key role in maintaining cell adhesion to ECM. In 2012, Su et al. found that *TA-p63*^{-/-} mice develop obesity: excess lipid accumulates in different tissues of *TA-p63*^{-/-} mice. These results revealed that *TA-p63* isoforms are crucial for regulating lipid metabolism (Su et al. 2012). Other studies showed that *Pltp* has roles besides lipid metabolism, such as the transfer of alpha-tocopherol (the most common form of *Vitamin E*) between different cellular compartments, which needs the presence of PLTP (Kostner et al. 1995). A study by Vuletic et al. (2003) showed that PLTP is expressed in neurons in the human brain but, unfortunately, they did not clarify the functions of PLTP protein.

Reviewing previous studies on *Pltp* shows that no role has been reported for this gene in any developmental processes. For the first time, Raj and Boughner's (2016) associated *Pltp* expression with odontogenesis and *TP63*, and my results support this finding by showing that *Pltp* is expressed in early stages of tooth development in the dental epithelium. More broadly, and perhaps more closely related to development than lipid metabolism, many studies explain the role of lipids in cell-cell adhesion (Sumigray and Lechler 2015), mediating epithelial cells interactions with each other, or other cell types, and mediating cell signaling (Colgan 2002; Serhan et al. 1996), and finally, in cell structure and differentiation (Wertz 1992). This knowledge suggests a possible link between *Pltp* function and *TP63* regulatory effect on *Pltp*. More to the point, this knowledge suggests that the expression of *Pltp* in dental epithelium is important for transferring lipids or other essential components. Also, this past work suggests that *Pltp* is essential for regulating lipids on the dental epithelium membrane and, consequently, epithelial adhesion to the ECM. Thus *Pltp* may mediate the physical bond between dental

epithelium and underlying mesenchyme so they can interact and signal to each other and support the normal differentiation of the dental epithelium.

Cbhl1 is well known for its role in the early stages of brain development (Miura et al. 2006) and this gene is widely expressed in the cerebellum (Slemmon et al. 1984, 1988). A study by Hirai et al. (2005) on a mouse mutant lacking *Cbhl1* reported that this gene is expressed in the post or presynaptic neurons of Purkinje cells and is important for the integrity and normal arrangement of cerebellar Purkinje cells (Hirai et al. 2005). Other studies revealed a potential role for *Cbhl1* in a signaling pathway that is essential for synapse plasticity and integrity, and found that CBLN1 is a secreted glycoprotein that acts as a signaling molecule in neurons (Miura et al. 2006). Related to my thesis work, perhaps *Cbhl1* is among the genes that, according to molecular and immunohistochemical analyses of the first molar in mice, helps regulate development of the first trigeminal dental nerve. This nerve reaches the dental epithelium at E10, and axons start growing toward the tooth at the early bud stage (Lumsden 1988; Kettunen et al. 2005). The dental nerve also innervates the developing tooth dental mesenchyme (Luukko et al. 2005). Epithelial-mesenchymal interactions along with different signaling molecules appear to regulate local innervation of the tooth. At early stages of tooth development, signals from dental epithelium predominantly mediate tooth innervation (Kettunen et al. 2005; Moe et al. 2012). Since my work showed that *Cbhl1* is expressed in epithelium (and at higher levels in the *TP63* mutant), perhaps *Cbhl1* helps regulate these earliest stages of tooth innervation.

My ISH results during placode and bud stages of tooth development showed for the first time that *Cbhl1* was significantly expressed in dental epithelium in the absence of *TP63*. Therefore, I propose that *Cbhl1* expression has a signaling role in mesenchymal-epithelial interactions. I suggest that the balance in the level of this gene is important for tooth

development and more specifically tooth innervation, and that in the absence of *TP63*, *Cbln1* over-expression perturbs signaling between epithelium and underlying mesenchyme in *TP63*-null mice and, consequently, perturbs nerve growth in dental mesenchyme.

Krt8 is expressed in simple or single layered internal epithelial cells and is expressed extensively in carcinomas. In contrast to my other three genes of interest, *Krt8* has been associated with *TP63*, where *TP63* repressed the expression of *Krt8* and *Krt18* (De Rosa et al. 2009). Related to this finding, a study on KRT8 levels in epidermal tissues (Truong et al. 2006) reported that down-regulation of ΔN -p63 resulted in the induction of KRT8. In addition, *Krt8* expression has been indirectly associated with *tenascin*, which is an extracellular matrix protein (Aufderheide and Ekblom in 1988). *Tenascin* is expressed in the mesenchyme around growing epithelia in the embryo and, more to the point here, regulates tooth development (Aufderheide and Ekblom 1988; Vainio et al. 1989). Also, *tenascin* is important for cell adhesion and cell interactions (Oberhauser et al. 1998). KRT8 has been associated with tumor progressions like cell adhesion and migration (Galarneau et al. 2007; Fortier et al. 2013). On the other hand, for the first time, my ISH results showed that *Krt8* expresses extensively in dental epithelium at early stages of tooth development in the *TP63*-null mouse. *TP63* is a tumor-suppressor and *Krt8* is involved in cancerous growth, which suggests that (as shown by past studies, noted above) *TP63* would logically suppress *Krt8*. Therefore, perhaps *Krt8* mediates dental epithelium cell adhesion and consequent interactions between epithelial cells and the underlying mesenchyme. In addition, possible functions for *Krt8* in apoptotic signaling were also suggested by Oshima in 2002. Programmed apoptosis is an important mechanism in bud formation and morphogenesis and shutting off the signaling centers during the tooth development. Also, a balance between cell division and apoptosis is essential for controlling the tooth shape and formation of the

appropriate tooth bud. Moreover, during the cell differentiation in an organ, apoptosis is the mechanism that controls the numbers cells (Matalova et al. 2004). From the above, another possibility is that *Krt8* regulates the apoptotic signals in dental epithelium cells that are going through differentiation.

In conclusion, based on the newly characterized *Fermt1*, *Pltp*, *Cbln1*, and *Krt8* expression domains - including the up-regulation effect of *TP63* on *Fermt1* and *Pltp*, and down-regulation effect of *TP63* on *Cbln1* and *Krt8* - during early stages of normal tooth development, I suggest that these four genes support the structural integrity, cell-cell adhesion, signaling and cross-talk between epithelial and underlying neural crest-derived mesenchymal cells. These four genes of interest along with *TP63* help mediate the epithelial-mesenchymal interactions that are required for dental epithelial cell maturation and proliferation during dental morphogenesis.

To explain the putative role for each of the genes of interest and the complicated mechanisms that they may help regulate during odontogenesis, further experiments are, of course, required. Although for some of these genes mutant organisms have been generated (Jiang et al. 1999; Ussar et al. 2008; Hirai et al. 2005), phenotype changes of teeth or during tooth development haven't been studied yet. Post translation and protein expression level profiling might be a good approach to test whether *TP63* interacts with any protein product of four new genes that I connected to *TP63*-mediated GRN (*Fermt1*, *Pltp*, *Cbln1*, and *Krt8*). Using techniques such as Chromatin Immunoprecipitation (ChIP) assay might be helpful to test whether *TP63* transcription factor directly regulates the expression of these genes (*Fermt1*, *Pltp*, *Cbln1*, and *Krt8*). Also, gene manipulation studies can help to understand the mechanism of function for each gene in odontogenesis. Functional experiments and study the phenotype changes of mutant organisms for each gene can lead us to more confident speculation about the function of these

genes. Other *in vitro* functional experiments and tissue engineering studies can help us to explain the role of these genes in epithelial structure, maturation and/or cell-cell cross-signaling.

Finally, since *TP63* is one of the major transcription factors required for initiating and regulating the development of epithelial cell layers, not only in mammals but also in other vertebrates, the proposed *TP63*-controlled gene regulatory network might provide broader insight about the evolution of the dentate jaw in vertebrates. However, so far, no published study has related my four candidate genes to odontogenesis in other vertebrates, although unpublished data suggests that at least some of these genes (*Pltp* and *Cbhl1*) are expressed in shark (small-spotted catshark) tooth organ tissues (Gareth Fraser, Univ. Sheffield, pers. comm.). In the future, performing gene expression studies on other dentate vertebrates, such as evolutionarily ancient animals like garfish, might help link a tooth specific *TP63*-controlled gene regulatory network to earlier dentate ancestors to test whether the role of a *TP63* GRN in odontogenesis is deeply conserved.

CHAPTER 5 - REFERENCES

- Albers JJ, Tu AY, Wolfbauer G, Cheung MC, Marcovina SM. 1996. Molecular biology of phospholipid transfer protein. *Current opinion in lipidology*, 7(2):88-93.
- Albers JJ, Vuletic S, Cheung MC. 2012. Role of plasma phospholipid transfer protein in lipid and lipoprotein metabolism. *Biochimica et biophysica acta*, 1821(3):345-57.
- Albers JJ, Wolfbauer G, Cheung MC, Day JR, Ching AF, Lok S, Tu AY. 1995. Functional expression of human and mouse plasma phospholipid transfer protein: effect of recombinant and plasma PLTP on HDL subspecies. *Biochimica et biophysica acta*, 1258(1):27-34.
- Aufderheide E, Ekblom P. 1988. Tenascin during gut development: appearance in the mesenchyme, shift in molecular forms, and dependence on epithelial-mesenchymal interactions. *The Journal of cell biology*, 107(6 Pt 1):2341-9.
- Belyi VA, Ak P, Markert E, Wang H, Hu W, Puzio-Kuter A, Levine AJ. 2010. The Origins and Evolution of the p53 Family of Genes. *Cold Spring Harbor perspectives in biology*, 2(6):a001198.
- Belyi VA, Levine AJ. 2009. One billion years of p53/p63/p73 evolution. *Proceedings of the National Academy of Sciences of the United States of America*, 106(42):17609-10.
- Boughner JC, Hallgrímsson B. 2008. Biological spacetime and the temporal integration of functional modules: a case study of dento-gnathic developmental timing. *Developmental dynamics: an official publication of the American Association of Anatomists*, 237(1):1-17.
- Calderwood DA, Campbell ID, Critchley DR. 2013. Talins and kindlins: partners in integrin-mediated adhesion. *Nature reviews. Molecular cell biology.*, 14(8):503-17.
- Carroll DK, Brugge JS, Attardi LD. 2007. p63, cell adhesion and survival. *Cell cycle*, 6(3):255-61.
- Chai Y, Bringas P Jr, Mogharei A, Shuler CF, Slavkin HC. 1998. PDGF-A and PDGFR- α regulate tooth formation via autocrine mechanism during mandibular morphogenesis in vitro. *Developmental dynamics: an official publication of the American Association of Anatomists*, 213(4):500-11.
- Chatterjee S, Boaz K. 2011. Molecular biology of odontogenesis. *Orofacial Sciences*, 3 (1):57-61.
- Cobourne MT, Sharpe PT. 2003. Tooth and jaw: molecular mechanisms of patterning in the first branchial arch. *Archives of oral biology*, 48(1):1-14.
- Colgan SP. 2002. Lipid mediators in epithelial cell-cell interactions. *CMLS, Cell. Mol. Life Sci*, 59: 754.

De Rosa L, Antonini D, Ferone G, Russo MT, Yu PB, Han R, Missero C. 2009. p63 Suppresses non-epidermal lineage markers in a bone morphogenetic protein-dependent manner via repression of Smad7. *The Journal of biological chemistry*, 284(44):30574-82.

Deans MR, Peterson JM, Wong GW. 2010. Mammalian Otolin: a multimeric glycoprotein specific to the inner ear that interacts with otoconial matrix protein Otoconin-90 and Cerebellin-1. *PloS one*, 5(9):e12765.

Fang J, Wang H, Liu Y, Ding F, Ni Y, Shao S. 2017. High KRT8 expression promotes tumor progression and metastasis of gastric cancer. *Cancer Sci.*, 108(2):178-186.

Fortier AM, Asselin E, Cadrin M. 2013. Keratin 8 and 18 loss in epithelial cancer cells increases collective cell migration and cisplatin sensitivity through claudin1 up-regulation. *The Journal of biological chemistry*, 288(16):11555-71.

Fraser GJ, Hulsey CD, Bloomquist RF, Uyesugi K, Manley NR, Streelman JT. 2009. An ancient gene network is co-opted for teeth on old and new jaws. *PLoS biology*, 7(2):e31.

Fukumoto S, Yamada Y. 2005. extracellular matrix regulates tooth morphogenesis. *Connective tissue research*, 46(4-5):220-6.

Galarneau L, Loranger A, Gilbert S, Marceau N. 2007. Keratins modulate hepatic cell adhesion, size and G1/S transition. *Experimental cell research*, 313(1):179-94.

Gyurján I, Sonderegger B, Naef F, Duboule D. 2011. Analysis of the dynamics of limb transcriptomes during mouse development. *BMC developmental biology*, 11:47.

Hardcastle Z, Mo R, Hui CC, Sharpe PT. 1998. The Shh signalling pathway in tooth development: defects in Gli2 and Gli3 mutants. *Development*, 125(15):2803-11.

Has C, Castiglia D, del Rio M, Diez MG, Piccinni E, Kiritsi D, Kohlhasse J, Itin P, Martin L, Fischer J, Zambruno G, Bruckner-Tuderman L. 2011. Kindler syndrome: extension of FERMT1 mutational spectrum and natural history. *Human mutation*, 32(11):1204-12.

Herz C, Aumailley M, Schulte C, Schlötzer-Schrehardt U, Bruckner-Tuderman L, Has C. 2006. Kindlin-1 is a phosphoprotein involved in regulation of polarity, proliferation, and motility of epidermal keratinocytes. *The Journal of biological chemistry*, 281(47):36082-90.

Hesse M, Magin TM, Weber K. 2001. Genes for intermediate filament proteins and the draft sequence of the human genome: novel keratin genes and a surprisingly high number of pseudogenes related to keratin genes 8 and 18. *Journal of cell science*, 114(Pt 14):2569-75.

Hirai H, Pang Z, Bao D, Miyazaki T, Li L, Miura E, Parris J, Rong Y, Watanabe M, Yuzaki M, Morgan JI. 2005. Cbln1 is essential for synaptic integrity and plasticity in the cerebellum. *Nature neuroscience*, 8(11):1534-4.

Hu X, Zhang S, Chen G, Lin C, Huang Z, Chen Y, Zhang Y. 2013. Expression of SHH signaling molecules in the developing human primary dentition. *BMC Dev Biol.*, 13:11.

- Jernvall J, Thesleff I. 2012. Tooth shape formation and tooth renewal: evolving with the same signals. *Development*, 139: 3487-3497.
- Jiang XC, Bruce C, Mar J, Lin M, Ji Y, Francone OL, Tall AR. 1999. Targeted mutation of plasma phospholipid transfer protein gene markedly reduces high-density lipoprotein levels. *The Journal of clinical investigation*, 103(6):907-14.
- Jobard F, Bouadjar B, Caux F, Hadj-Rabia S, Has C, Matsuda F, Weissenbach J, Lathrop M, Prud'homme JF, Fischer J. 2003. Identification of mutations in a new gene encoding a FERM family protein with a pleckstrin homology domain in Kindler syndrome. *Human molecular genetics*, 12(8):925-35.
- Joerger AC, Rajagopalan S, Natan E, Veprintsev DB, Robinson CV, Fersht AR. 2009. Structural evolution of p53, p63, and p73: implication for heterotetramer formation. *Proc Natl Acad Sci U S A*, 106(42):17705-10.
- Kettunen P, Løes S, Furmanek T, Fjeld K, Kvinnsland IH, Behar O, Yagi T, Fujisawa H, Vainio S, Taniguchi M, Luukko K. 2005. Coordination of trigeminal axon navigation and patterning with tooth organ formation: epithelial-mesenchymal interactions, and epithelial Wnt4 and Tgfbeta1 regulate semaphorin 3a expression in the dental mesenchyme. *Development*, 132(2):323-34.
- Koster MI, Kim S, Mills AA, DeMayo FJ, Roop DR. 2004. p63 is the molecular switch for initiation of an epithelial stratification program. *Genes & development*, 18(2): 126–131.
- Kostner GM, Oettl K, Jauhainen M, Ehnholm C, Esterbauer H, Dieplinger H. 1995. Human plasma phospholipid transfer protein accelerates exchange/transfer of alpha-tocopherol between lipoproteins and cells. *The Biochemical journal*, 305 (Pt 2):659-67.
- Kouwenhoven EN, van Bokhoven H, Zhou H. 2015. Gene regulatory mechanisms orchestrated by p63 in epithelial development and related disorders. *Biochimica et biophysica acta*, 1849(6):590-600.
- Koyama E, Yamaai T, Iseki S, Ohuchi H, Nohno T, Yoshioka H, Hayashi Y, Leatherman JL, Golden EB, Noji S, Pacifici M. 1996. Polarizing activity, Sonic hedgehog, and tooth development in embryonic and postnatal mouse. *Developmental dynamics*, 206(1):59-72.
- Lagrost L, Desrumaux C, Masson D, Deckert V, Gambert P. 1998. Structure and function of the plasma phospholipid transfer protein. *Current opinion in lipidology*, 9(3):203-9.
- Laurikkala J, Mikkola ML, James M, Tummers M, Mills AA, Thesleff I. 2006. p63 regulates multiple signalling pathways required for ectodermal organogenesis and differentiation. *Development*, 133(8):1553-63.
- Lee SH, Bédard O, Buchtová M, Fu K, Richman JM. 2004. A new origin for the maxillary jaw. *Developmental biology*, 276(1):207-24.

- Lumsden AG. 1988. Spatial organization of the epithelium and the role of neural crest cells in the initiation of the mammalian tooth germ. *Development*, 103 Suppl:155-69.
- Luukko K, Kettunen P. 2014. Coordination of tooth morphogenesis and neuronal development through tissue interactions: lessons from mouse models. *Experimental cell research*, 325(2):72-7.
- Luukko K, Kvinnsland IH, Kettunen P. 2005. Tissue interactions in the regulation of axon pathfinding during tooth morphogenesis. *Dev Dyn.*, 234(3):482-8.
- Makino T, Yamasaki M, Takeno A, Shirakawa M, Miyata H, Takiguchi S, Nakajima K, Fujiwara Y, Nishida T, Matsuura N, Mori M, Doki Y. 2009. Cytokeratins 18 and 8 are poor prognostic markers in patients with squamous cell carcinoma of the oesophagus. *British journal of cancer*, 101(8):1298-306.
- Malinin NL, Plow EF, Byzova TV. 2010. Kindlins in FERM adhesion. *Blood*, 115(20):4011-7.
- Márquez MG, Favale NO, Leocata Nieto F, Pescio LG, Sterin-Speziale N. 2012. Changes in membrane lipid composition cause alterations in epithelial cell-cell adhesion structures in renal papillary collecting duct cells. *Biochim Biophys Acta.*, 1818(3):491-501.
- Márquez MG, Nieto FL, Fernández-Tome MC, Favale NO, Sterin-Speziale N. 2008. Membrane lipid composition plays a central role in the maintenance of epithelial cell adhesion to the extracellular matrix. *Lipids*, 43(4):343-52.
- Matalova E, Tucker AS, Sharpe PT. 2004. Death in the life of a tooth. *J Dent Res.*, 83(1):11-6.
- Matsuura T, Kawata VK, Nagoshi H, Tomooka Y, Sasaki K, Ikawa S. 2012. Regulation of proliferation and differentiation of mouse tooth germ epithelial cells by distinct isoforms of p51/p63. *Archives of oral biology*, 57(8):1108-15.
- McCollum M, Sharpe PT. 2001. Evolution and development of teeth. *Journal of Anatomy*, 199(Pt 1-2):153–159.
- Mills AA, Zheng B, Wang XJ, Vogel H, Roop DR, Bradley A. 1999. p63 is a p53 homologue required for limb and epidermal morphogenesis. *Nature*, 398(6729):708-13.
- Mitsiadis TA, Graf D, Luder H, Gridley T, Bluteau G. 2010. BMPs and FGFs target Notch signalling via jagged 2 to regulate tooth morphogenesis and cytodifferentiation. *Development*, 137(18): 3025–3035.
- Miura E, Iijima T, Yuzaki M, Watanabe M. 2006. Distinct expression of Cbln family mRNAs in developing and adult mouse brains. *The European journal of neuroscience*, 24(3):750-60.
- Moe K, Sijaona A, Shrestha A, Kettunen P, Taniguchi M, Luukko K. 2012. Semaphorin 3A controls timing and patterning of the dental pulp innervation. *Differentiation*, 84(5):371-9.
- Oberhauser AF, Marszalek PE, Erickson HP, Fernandez JM. 1998. The molecular elasticity of the extracellular matrix protein tenascin. *Nature*, 393, 181–185.

O'Brien KD, Vuletic S, McDonald TO, Wolfbauer G, Lewis K, Tu AY, Marcovina S, Wight TN, Chait A, Albers JJ. 2003. Cell-associated and extracellular phospholipid transfer protein in human coronary atherosclerosis. *Circulation*, 108(3):270-4.

Odutuga AA, Prout RE. 1975. Fatty acid composition of carious molar enamel and dentine from rats deficient in essential fatty acids. *Archives of oral biology*, 20(1):49-51.

Oshima RG. 2002. Apoptosis and keratin intermediate filaments. *Cell death & differentiation*, 9(5):486-92.

Owen R. 1840-1845. *Odontography; or, a Treatise on the Comparative Anatomy of the Teeth. Their Physiological Relations, Mode of Development, and Microscopic Structure, in the Vertebrate Animals. Two Volumes (Text & Atlas)*. London: Hippolyte Bailliere.

Palombo R, Porta G, Bruno E, Provero P, Serra V, Neduri K, Viziano A, Alessandrini M, Micarelli A, Ottaviani F, Melino G, Terrinon A. 2015. OTX2 regulates the expression of TAp63 leading to macular and cochlear neuroepithelium development. *Aging*, 7(11): 928–936.

Pansky B. 1982. Development Of The Teeth. In P. B, *Review of Medical Embryology* (pp. 77-78). Toledo: Copyright © 1982, Ben Pansky.

Paradis MR, Raj MT, Boughner JC. 2013. Jaw growth in the absence of teeth: the developmental morphology of edentulous mandibles using the p63 mouse mutant. *Evolution & Development*, 15(4):268-79.

Pearson MA, Reczek D, Bretscher A, Karplus PA. 2000. Structure of the ERM protein moesin reveals the FERM domain fold masked by an extended actin binding tail domain. *Cell*, 101(3):259-70.

Pispa J, Thesleff I. 2003. Mechanisms of ectodermal organogenesis. *Developmental biology*, 262(2):195-205.

Raj MT, Boughner JC. 2016. Detangling the evolutionary developmental integration of dentate jaws: evidence that a p63 gene network regulates odontogenesis exclusive of mandible morphogenesis. *Evolution & development*, 18(5-6):317-323.

Rücklin M, Donoghue P, Johanson Z, Trinajstić K, Marone F, Stampanoni M. 2012. Development of teeth and jaws in the earliest jawed vertebrates. *Nature*, 491:748–751.

Rufini A, Weil M, McKeon F, Barlattani A, Melino G, Candi E. 2006. p63 protein is essential for the embryonic development of vibrissae and teeth. *Biochemical and biophysical research communications*, 340(3):737-41.

Serhan CN, Haeggström JZ, Leslie CC. 1996. Lipid mediator networks in cell signaling: update and impact of cytokines. *FASEB journal*, 10(10):1147-58.

Siegel DH, Ashton GH, Penagos HG, Lee JV, Feiler HS, Wilhelmsen KC, South AP, Smith FJ, Prescott AR, Wessagowit V, Oyama N, Akiyama M, Al Aboud D, Al Aboud K, Al Githami A,

- Al Hawsawi K, Al Ismaily A, Al-Suwaid R, Atherton DJ, Caputo R, Fine JD, Frieden. 2003. Loss of kindlin-1, a human homolog of the *Caenorhabditis elegans* actin-extracellular-matrix linker protein UNC-112, causes Kindler syndrome. *American journal of human genetics*, 73(1):174-87.
- Slemmon JR, Blacher R, Danho W, Hempstead JL, Morgan JI. 1984. Isolation and sequencing of two cerebellum-specific peptides. *Proceedings of the National Academy of Sciences of the United States of America*, 81(21):6866-70.
- Slemmon JR, Goldowitz D, Blacher R, Morgan JI. 1988. Evidence for the transneuronal regulation of cerebellin biosynthesis in developing Purkinje cells. *Journal of Neuroscience*, 8 (12) 4603-4611.
- Su X, Gi YJ, Chakravarti D, Chan IL, Zhang A, Xia X, Tsai KY, Flores ER. 2012. TAp63 is a master transcriptional regulator of lipid and glucose metabolism. *Cell metabolism*, 16(4):511-25.
- Sumigay KD, Lechler T. 2015. Cell adhesion in epidermal development and barrier formation. *Current topics in developmental biology*, 112:383-414.
- Tan HS, Jiang WH, He Y, Wang DS, Wu ZJ, Wu DS, Gao L, Bao Y, Shi JZ, Liu B, Ma LJ, Wang LH. 2017. KRT8 upregulation promotes tumor metastasis and is predictive of a poor prognosis in clear cell renal cell carcinoma. *Oncotarget*, 8(44):76189-76203.
- Thesleff I. 2003. Epithelial-mesenchymal signalling regulating tooth morphogenesis. *Journal of Cell Science*, 116: 1647-1648.
- Thesleff I. 2006. The genetic basis of tooth development and dental defects. *American Journal of Medical Genetics. Part A*, 140(23):2530-5.
- Thesleff I, Ekblom P. 1984. Distribution of keratin and laminin in ameloblastoma. Comparison with developing tooth and epidermoid carcinoma. *Journal of Oral Pathology & Medicine*, 13(1):85-96.
- Thesleff I, Partanen AM, Vainio S. 1991. Epithelial-mesenchymal interactions in tooth morphogenesis: the roles of extracellular matrix, growth factors, and cell surface receptors. *Journal of craniofacial genetics and developmental biology*, 11(4):229-37.
- Thesleff I, Tummers M. 2009. Tooth organogenesis and regeneration. Cambridge: StemBook.
- Thomason HA, Zhou H, Kouwenhoven EN, Dotto GP, Restivo G, Nguyen BC, Little H, Dixon MJ, van Bokhoven H, Dixon J. 2010. Cooperation between the transcription factors p63 and IRF6 is essential to prevent cleft palate in mice. *The Journal of clinical investigation*, 120(5):1561-9.
- Truong AB, Kretz M, Ridky TW, Kimmel R, Khavari PA. 2006. p63 regulates proliferation and differentiation of developmentally mature keratinocytes. *Genes & development*, 20(22):3185-97.

- Urade Y, Oberdick J, Molinar-Rode R, Morgan JJ. 1991. Precerebellin is a cerebellum-specific protein with similarity to the globular domain of complement C1q B chain. PNAS, 88(3):1069-73.
- Ussar S, Moser M, Widmaier M, Rognoni E, Harrer C, Genzel-Boroviczeny O, Fässler R. 2008. Loss of Kindlin-1 Causes Skin Atrophy and Lethal Neonatal Intestinal Epithelial Dysfunction. PLoS genetics., 4(12): e1000289.
- Vainio S, Jalkanen M, Thesleff I. 1989. Syndecan and tenascin expression is induced by epithelial-mesenchymal interactions in embryonic tooth mesenchyme. The Journal of cell biology, 108(5):1945-53.
- Vuletic S, Jin LW, Marcovina SM, Peskind ER, Moller T, Albers JJ. 2003. Widespread distribution of PLTP in human CNS: evidence for PLTP synthesis by glia and neurons, and increased levels in Alzheimer's disease. Journal of lipid research, 44(6):1113-23.
- Wertz PW. 1992. Epidermal lipids. Seminars in dermatology, 11(2):106-13.
- Yang A, Kaghad M, Caput D, McKeon F. 2002. On the shoulders of giants: p63, p73 and the rise of p53. Trends in genetics: TIG, 18(2):90-5.
- Yang A, Kaghad M, Wang Y, Gillett E, Fleming MD, Dötsch V, Andrews NC, Caput D, McKeon F. 1998. p63, a p53 homolog at 3q27-29, encodes multiple products with transactivating, death-inducing, and dominant-negative activities. Molecular cell, 2(3):305-16.
- Yang A, Schweitzer R, Sun D, Kaghad M, Walker N, Bronson RT, Tabin C, Sharpe A, Caput D, Crum C, McKeon F. 1999. p63 is essential for regenerative proliferation in limb, craniofacial and epithelial development. Nature, 398(6729):714-8.
- Yoh K, Prywes R. 2015. Pathway Regulation of p63, a Director of Epithelial Cell Fate. Frontiers in endocrinology, 6: 51.

Appendix A

Sequencing results from Eurofins Genomics company blasted against published sequences of mRNA in Basic Local Alignment Search Tool (Standard Nucleotide BLAST:

https://blast.ncbi.nlm.nih.gov/Blast.cgi?PROGRAM=blastn&PAGE_TYPE=BlastSearch&LINK_LOC=blasthome)

Sonic hedgehog (*Shh*) synthesized anti-Sense probe with T7 polymerase:

Mus musculus sonic hedgehog (*Shh*), mRNA

Sequence ID: [NM_009170.3](#) Length: 2727 Number of Matches: 1

Range 1: 339 to 1156 [GenBank](#) [Graphics](#) ▼ Next Match ▲ Previous Match

Score	Expect	Identities	Gaps	Strand
1506 bits(815)	0.0	818/819(99%)	1/819(0%)	Plus/Minus
Query 25	AGCAGGTGCGCGGCGGTGAGCAGCAGGCGCTCGCGCGGCTCCAGCGTCTCGATCACGTAG	84		
Sbjct 1156	AGCAGGTGCGCGGCGGTGAGCAGCAGGCGCTCGCGCGGCTCCAGCGTCTCGATCACGTAG	1097		
Query 85	AAGACCTTCTTGGCGCCTTCGTGCGGTCAGGAAGGTGAGGAAGTCGCTGTACAGCAGC	144		
Sbjct 1096	AAGACCTTCTTGGCGCCTTCGTGCGGTCAGGAAGGTGAGGAAGTCGCTGTACAGCAGC	1037		
Query 145	CGGCCCTGGTCGTCAGCCGCCAGCAGCGGCTCTCCGGGACGTAAGTCCTTACCAGCTTG	204		
Sbjct 1036	CGGCCCTGGTCGTCAGCCGCCAGCAGCGGCTCTCCGGGACGTAAGTCCTTACCAGCTTG	977		
Query 205	GTGCCGCCCTGCTCCAGGTGCACGGTGCGGGATCCCGGAAACAGCCGCCGGATTGGCC	264		
Sbjct 976	GTGCCGCCCTGCTCCAGGTGCACGGTGCGGGATCCCGGAAACAGCCGCCGGATTGGCC	917		
Query 265	GCCACGGAGTTCTCTGCTTTCACAGAACAGTGGATGTGAGCTTTGGATTCATAGTAGACC	324		
Sbjct 916	GCCACGGAGTTCTCTGCTTTCACAGAACAGTGGATGTGAGCTTTGGATTCATAGTAGACC	857		
Query 325	CAGTCGAAACCTGCTTCCACAGCCAGGCGAGCCAGCATGCCGTACTTGCTGCGGTCCCGG	384		
Sbjct 856	CAGTCGAAACCTGCTTCCACAGCCAGGCGAGCCAGCATGCCGTACTTGCTGCGGTCCCGG	797		
Query 385	TCGGACGTGGTGATGTCCACTGCTCGACCCATAGTGTAGAGACTCCTCTGAATGATGG	444		
Sbjct 796	TCGGACGTGGTGATGTCCACTGCTCGACCCATAGTGTAGAGACTCCTCTGAATGATGG	737		
Query 445	CCGTCTCATCCAGCCCTCGGTCACTCGCAGCTTCACTCCAGGCCACTGGTTTCATCACA	504		
Sbjct 736	CCGTCTCATCCAGCCCTCGGTCACTCGCAGCTTCACTCCAGGCCACTGGTTTCATCACA	677		
Query 505	GAGATGGCCAAGGCATTTAACTTGCTTTGCACCTCTGAGTCATCAGCCGGTCTGCTCCC	564		
Sbjct 676	GAGATGGCCAAGGCATTTAACTTGCTTTGCACCTCTGAGTCATCAGCCGGTCTGCTCCC	617		
Query 565	GTGTTTTCTCATCCTTAAATATGATGTCGGGGTTGTAATTGGGGGTGAGTTCTTTAAA	624		
Sbjct 616	GTGTTTTCTCATCCTTAAATATGATGTCGGGGTTGTAATTGGGGG-TGAGTTCTTTAAA	558		
Query 625	TCGTTTCGGAGTTTCTTGATCTTCCCTTCATATCTGCCGCTGGCCCCAGGGTCTTCTC	684		
Sbjct 557	TCGTTTCGGAGTTTCTTGATCTTCCCTTCATATCTGCCGCTGGCCCCAGGGTCTTCTC	498		
Query 685	GGCTACGTTGGGAATAAACTGCTTGTAGGCTAAAGGGGTGAGTTTGGGGTGCCGCCT	744		
Sbjct 497	GGCTACGTTGGGAATAAACTGCTTGTAGGCTAAAGGGGTGAGTTTGGGGTGCCGCCT	438		
Query 745	CTTTCCAAACCCCTGCCGGGCCACAGGCCAGCCGGGGCACACCAGCAGCGAGGAAGC	804		
Sbjct 437	CTTTCCAAACCCCTGCCGGGCCACAGGCCAGCCGGGGCACACCAGCAGCGAGGAAGC	378		
Query 805	AAGGATCACCAGAAAACATCTGGCCAGCAGCAGCAGCAT	843		
Sbjct 377	AAGGATCACCAGAAAACATCTGGCCAGCAGCAGCAGCAT	339		

Sonic hedgehog (*Shh*) synthesized Sense probe with T3 polymerase:

Mus musculus sonic hedgehog (*Shh*), mRNA

Sequence ID: [NM_009170.3](#) Length: 2727 Number of Matches: 1

Range 1: 358 to 1187 [GenBank](#) [Graphics](#)

▼ Next Match ▲ Previous Match

Score	Expect	Identities	Gaps	Strand
1533 bits(830)	0.0	830/830(100%)	0/830(0%)	Plus/Plus
Query 14	GATGTTTTCTGGTGATCCTTGCTTCCTCGCTGCTGGTGTGCCCCGGGCTGGCCTGTGGGC			73
Sbjct 358	GATGTTTTCTGGTGATCCTTGCTTCCTCGCTGCTGGTGTGCCCCGGGCTGGCCTGTGGGC			417
Query 74	CCGGCAGGGGGTTTGGAAAGAGGCGGCACCCCAAAAAGCTGACCCCTTTAGCCTACAAGC			133
Sbjct 418	CCGGCAGGGGGTTTGGAAAGAGGCGGCACCCCAAAAAGCTGACCCCTTTAGCCTACAAGC			477
Query 134	AGTTTATTTCCCAACGTAGCCGAGAAGACCCTAGGGGCCAGCGGCAGATATGAAGGGAAGA			193
Sbjct 478	AGTTTATTTCCCAACGTAGCCGAGAAGACCCTAGGGGCCAGCGGCAGATATGAAGGGAAGA			537
Query 194	TCACAAGAAACTCCGAACGATTTAAGGAACTCACCCCAATTACAACCCCGACATCATAT			253
Sbjct 538	TCACAAGAAACTCCGAACGATTTAAGGAACTCACCCCAATTACAACCCCGACATCATAT			597
Query 254	TTAAGGATGAGGAAAAACACGGGAGCAGACCGGCTGATGACTCAGAGGTGCAAAGACAAGT			313
Sbjct 598	TTAAGGATGAGGAAAAACACGGGAGCAGACCGGCTGATGACTCAGAGGTGCAAAGACAAGT			657
Query 314	TAAATGCCTTGGCCATCTCTGTGATGAACCAAGTGGCCTGGAGTGAAGCTGCGAGTGACCG			373
Sbjct 658	TAAATGCCTTGGCCATCTCTGTGATGAACCAAGTGGCCTGGAGTGAAGCTGCGAGTGACCG			717
Query 374	AGGGCTGGGATGAGGACGGCCATCATTAGAGGAGTCTCTACACTATGAGGGTCGAGCAG			433
Sbjct 718	AGGGCTGGGATGAGGACGGCCATCATTAGAGGAGTCTCTACACTATGAGGGTCGAGCAG			777
Query 434	TGGACATCACCAAGTCCGACCGGGACCGCAGCAAGTACGGCATGCTGGCTCGCCTGGCTG			493
Sbjct 778	TGGACATCACCAAGTCCGACCGGGACCGCAGCAAGTACGGCATGCTGGCTCGCCTGGCTG			837
Query 494	TGGAAGCAGGTTTCGACTGGGTCTACTATGAATCCAAAGCTCACATCCACTGTTCTGTGA			553
Sbjct 838	TGGAAGCAGGTTTCGACTGGGTCTACTATGAATCCAAAGCTCACATCCACTGTTCTGTGA			897
Query 554	AAGCAGAGAACTCCGTGGCGGCCAAATCCGGCGGCTGTTTCCCGGGATCCGCCACCGTGC			613
Sbjct 898	AAGCAGAGAACTCCGTGGCGGCCAAATCCGGCGGCTGTTTCCCGGGATCCGCCACCGTGC			957
Query 614	ACCTGGAGCAGGGCGGCACCAAGCTGGTGAAGGACTTACGTCCCGGAGACCGCGTGTGG			673
Sbjct 958	ACCTGGAGCAGGGCGGCACCAAGCTGGTGAAGGACTTACGTCCCGGAGACCGCGTGTGG			1017
Query 674	CGGCTGACGACCAAGGCGCGCTGCTGTACAGCGACTTCCTCACCTTCCTGGACCGCGACG			733
Sbjct 1018	CGGCTGACGACCAAGGCGCGCTGCTGTACAGCGACTTCCTCACCTTCCTGGACCGCGACG			1077
Query 734	AAGGCGCCAAGAAGGTCTTCTACGTGATCGAGACGCTGGAGCCGCGAGCGCCTGCTGC			793
Sbjct 1078	AAGGCGCCAAGAAGGTCTTCTACGTGATCGAGACGCTGGAGCCGCGAGCGCCTGCTGC			1137
Query 794	TCACCGCCGCGCACCTGCTCTTCGTGGCGCCGCACAACGACTCGGGGCCC			843
Sbjct 1138	TCACCGCCGCGCACCTGCTCTTCGTGGCGCCGCACAACGACTCGGGGCCC			1187

Tumor Protein 63 (TP63) synthesized anti-Sense probe with T7 polymerase:

Mus musculus transformation related protein 63 (Trp63), transcript variant 5, mRNA

Sequence ID: [NM_001127264.1](#) Length: 4707 Number of Matches: 1

Range 1: 3927 to 4417 [GenBank](#) [Graphics](#)

▼ Next Match ▲ Previous Match

Score	Expect	Identities	Gaps	Strand
893 bits(483)	0.0	487/491(99%)	0/491(0%)	Plus/Minus
Query 20	GTATTCAGGGGGGATATCAAGAAAACAAAAGCTAACTGGATTAACAAAGAGAATCCTGCT	79		
Sbjct 4417	GTATTCAGGGGGGATATCAAGAAAACAAAAGCTAACTGGATTAACAAAGAGAATCCTGCT	4358		
Query 80	TTCTATCCTATCTGCTTCACCACCAAGTGAAGGAATCCCATTCTCCACTGAGAGGCATCC	139		
Sbjct 4357	TTCTATCCTATCTGCTTCACCACCAAGTGAAGGAATCCCATTCTCCACTGAGAGGCATCC	4298		
Query 140	AGCAGATGTCTGTTCTCTGTGTTCTTCCCCACAGCTCTGGCTATTNANACACTAAACACT	199		
Sbjct 4297	AGCAGATGTCTGTTCTCTGTGTTCTTCCCCACAGCTCTGGCTATTNANACACTAAACACT	4238		
Query 200	GGTGTGAGGAGACAAACTGTGCCTACCTATGGCTAATGCCAAAATCATCAGATACAGTAC	259		
Sbjct 4237	GGTGTGAGGAGACAAACTGTGCCTACCTATGGCTAATGCCAAAATCATCAGATACAGTAC	4178		
Query 260	AGGAATTTCCANNGTCCCTAGTGCCACCTAAATAGTGCTGAAATGCCACAGAGTCCCCTGT	319		
Sbjct 4177	AGGAATTTCCAGAGTCCCTAGTGCCACCTAAATAGTGCTGAAATGCCACAGAGTCCCCTGT	4118		
Query 320	GCCACACCAACACTGCTGAAACAGCCCCAAATACTTACAACACACAGGAAGCCATTTGTCT	379		
Sbjct 4117	GCCACACCAACACTGCTGAAACAGCCCCAAATACTTACAACACACAGGAAGCCATTTGTCT	4058		
Query 380	TCCTAACATGGCTAAGACACAGCTTTCTTCTCCACCCATTGAATTTGTAAAGCTGTGAGT	439		
Sbjct 4057	TCCTAACATGGCTAAGACACAGCTTTCTTCTCCACCCATTGAATTTGTAAAGCTGTGAGT	3998		
Query 440	TTGTTACAGAAGTTAATGATGCTTATCATTATTTAAACACAACAAAATGTTGAAATTAAG	499		
Sbjct 3997	TTGTTACAGAAGTTAATGATGCTTATCATTATTTAAACACAACAAAATGTTGAAATTAAG	3938		
Query 500	GACTCATTTGC	510		
Sbjct 3937	GACTCATTTGC	3927		

Tumor Protein 63 (TP63) synthesized Sense probe with T3 polymerase:

Mus musculus transformation related protein 63 (Trp63), transcript variant 5, mRNA

Sequence ID: [NM_001127264.1](#) Length: 4707 Number of Matches: 1

Range 1: 3933 to 4446 [GenBank](#) [Graphics](#)

▼ Next Match ▲ Previous Match

Score	Expect	Identities	Gaps	Strand
946 bits(512)	0.0	513/514(99%)	0/514(0%)	Plus/Plus
Query 24	GAGTCCTTAATTTT	CANCAATTTTGTGTGTTTAAATAATGATAAGCATCATTAACCTTCTGT	83	
Sbjct 3933	GAGTCCTTAATTTT	CAACATTTTGTGTGTTTAAATAATGATAAGCATCATTAACCTTCTGT	3992	
Query 84	AACAAACTCACAGCTTTACAAATTC	CAATGGGTGGAGAAGAAAGCTGTGTCTTAGCCATGT	143	
Sbjct 3993	AACAAACTCACAGCTTTACAAATTC	CAATGGGTGGAGAAGAAAGCTGTGTCTTAGCCATGT	4052	
Query 144	TAGGAAGACAAATGGCTTCCTGTGTGTTGTAAGTATTTGGGCTGTTTCAGCAGTGTGGT	203		
Sbjct 4053	TAGGAAGACAAATGGCTTCCTGTGTGTTGTAAGTATTTGGGCTGTTTCAGCAGTGTGGT	4112		
Query 204	GTGGCACAGGGGACTCTGTGGCATTTCAGCACTATTTAGGTGGCACTAGGGACTCTGAAA	263		
Sbjct 4113	GTGGCACAGGGGACTCTGTGGCATTTCAGCACTATTTAGGTGGCACTAGGGACTCTGAAA	4172		
Query 264	TTCCTGTACTGTATCTGATGATTTTGGCATTAGCCATAGGTAGGCACAGTTTGTCTCCTC	323		
Sbjct 4173	TTCCTGTACTGTATCTGATGATTTTGGCATTAGCCATAGGTAGGCACAGTTTGTCTCCTC	4232		
Query 324	ACACCAGTGTTTAGTGTGTGAATAGCCAGAGCTGTGGGGAAGAACACAGAGAACAGACAT	383		
Sbjct 4233	ACACCAGTGTTTAGTGTGTGAATAGCCAGAGCTGTGGGGAAGAACACAGAGAACAGACAT	4292		
Query 384	CTGCTGGATGCCTCTCAGTGGAGAATGGGATTCTTCACTTGGTGGTGAAGCAGATAGGA	443		
Sbjct 4293	CTGCTGGATGCCTCTCAGTGGAGAATGGGATTCTTCACTTGGTGGTGAAGCAGATAGGA	4352		
Query 444	TAGAAAGCAGGATTCTCTTTGTTAATCCAGTTAGCTTTTGTCTTCTTGATATCCCCCTG	503		
Sbjct 4353	TAGAAAGCAGGATTCTCTTTGTTAATCCAGTTAGCTTTTGTCTTCTTGATATCCCCCTG	4412		
Query 504	AATACGTTGAGTATGAGAGATATGTGGGTTTTTT	537		
Sbjct 4413	AATACGTTGAGTATGAGAGATATGTGGGTTTTTT	4446		

Fermitin 1 (*Fermt1*) synthesized anti-Sense probe with T7 polymerase:

PREDICTED: Mus musculus fermitin family member 1 (*Fermt1*), transcript variant X3, mRNA

Sequence ID: [XM_017318210.1](#) Length: 4855 Number of Matches: 1

Range 1: 1639 to 2333 [GenBank](#) [Graphics](#)

▼ Next Match ▲ Previous Match

Score	Expect	Identities	Gaps	Strand
1280 bits(693)	0.0	694/695(99%)	0/695(0%)	Plus/Minus
Query 22	AGGNCCTCATCGAGCGTTTCGTTTTGGTCCTTGGATCGGGTGGACAAGAAGATGTAGCCA	81		
Sbjct 2333	AGGTCTCATCGAGCGTTTCGTTTTGGTCCTTGGATCGGGTGGACAAGAAGATGTAGCCA	2274		
Query 82	CCAATGTACTCATGGACAATCTTGCAATCTGCACCTAGGCAGGTGAATGCGATGGAGACG	141		
Sbjct 2273	CCAATGTACTCATGGACAATCTTGCAATCTGCACCTAGGCAGGTGAATGCGATGGAGACG	2214		
Query 142	TTTTGGTCAAACCTCGATTGCCACCTGCCGGATTTCCAGTTGACATTCCTGCTTCATA	201		
Sbjct 2213	TTTTGGTCAAACCTCGATTGCCACCTGCCGGATTTCCAGTTGACATTCCTGCTTCATA	2154		
Query 202	TTGGCGAATCTCCACGTTGTAACCTGGTATCCAGTGACCGCATCGATTCTAATCAACCTG	261		
Sbjct 2153	TTGGCGAATCTCCACGTTGTAACCTGGTATCCAGTGACCGCATCGATTCTAATCAACCTG	2094		
Query 262	TTGTATGCAACTCCAGGATGTCATCTTTTTGCTTCCTTTAAATCTGACAAGGTAGTAG	321		
Sbjct 2093	TTGTATGCAACTCCAGGATGTCATCTTTTTGCTTCCTTTAAATCTGACAAGGTAGTAG	2034		
Query 322	GTGAGGCCGAACCTCAGGTAAGGATTGCCAGGCCTGGATGAACTGCAGTTTGGCTTCGACC	381		
Sbjct 2033	GTGAGGCCGAACCTCAGGTAAGGATTGCCAGGCCTGGATGAACTGCAGTTTGGCTTCGACC	1974		
Query 382	AGAGGCATCTGGGCTACGTTATGGTGAGCTTCCAGGATCCGGGCCGCCAGCTGTTTAGAC	441		
Sbjct 1973	AGAGGCATCTGGGCTACGTTATGGTGAGCTTCCAGGATCCGGGCCGCCAGCTGTTTAGAC	1914		
Query 442	TTGTGCTTTTTTGCACAGCAGGGCGATACTAAACATTCCGGGTTTCATATCCATGTTTTCA	501		
Sbjct 1913	TTGTGCTTTTTTGCACAGCAGGGCGATACTAAACATTCCGGGTTTCATATCCATGTTTTCA	1854		
Query 502	AGACTGGAAGCCACCAGAGGTGATGAGTTCCGGTTTTTCATCTTGAGAAACGAAAGGATG	561		
Sbjct 1853	AGACTGGAAGCCACCAGAGGTGATGAGTTCCGGTTTTTCATCTTGAGAAACGAAAGGATG	1794		
Query 562	CTGATGACCTCTGGCTGATAGGAGCTGTCTGCCATAGTTTTACCCCTTCGATGCCAAGATG	621		
Sbjct 1793	CTGATGACCTCTGGCTGATAGGAGCTGTCTGCCATAGTTTTACCCCTTCGATGCCAAGATG	1734		
Query 622	CAGGCAGCCATCCATCGGGCATATTGATCCTCATGGTCACATCTCAAGTACACTTCATTC	681		
Sbjct 1733	CAGGCAGCCATCCATCGGGCATATTGATCCTCATGGTCACATCTCAAGTACACTTCATTC	1674		
Query 682	ATACCATCAGCAACGGGGATTAGTAACCTTGATTCC	716		
Sbjct 1673	ATACCATCAGCAACGGGGATTAGTAACCTTGATTCC	1639		

Fermitin 1 (*Fermt1*) synthesized Sense probe with T3 polymerase:

PREDICTED: Mus musculus fermitin family member 1 (Fermt1), transcript variant X3, mRNA

Sequence ID: [XM_017318210.1](#) Length: 4855 Number of Matches: 1

Range 1: 1662 to 2364 [GenBank](#) [Graphics](#)

▼ Next Match ▲ Previous Match

Score	Expect	Identities	Gaps	Strand
1299 bits(703)	0.0	703/703(100%)	0/703(0%)	Plus/Plus
Query 10	TGCTGATGGTATGAATGAAGTGTACTTGAGATGTGACCATGAGGATCAATATGCCCGATG	69		
Sbjct 1662	TGCTGATGGTATGAATGAAGTGTACTTGAGATGTGACCATGAGGATCAATATGCCCGATG	1721		
Query 70	GATGGCTGCCTGCATCTTGGCATCGAAGGGTAAACTATGGCAGACAGCTCCTATCAGCC	129		
Sbjct 1722	GATGGCTGCCTGCATCTTGGCATCGAAGGGTAAACTATGGCAGACAGCTCCTATCAGCC	1781		
Query 130	AGAGGTCATCAGCATCCTTTCTGTTTCTCAAGATGAAAAACCGGAACATCACCTCTGGT	189		
Sbjct 1782	AGAGGTCATCAGCATCCTTTCTGTTTCTCAAGATGAAAAACCGGAACATCACCTCTGGT	1841		
Query 190	GGCTTCCAGTCTTGAAACATGGATATGAACCCGGAATGTTTAGTATCGCCCTGCTGTGC	249		
Sbjct 1842	GGCTTCCAGTCTTGAAACATGGATATGAACCCGGAATGTTTAGTATCGCCCTGCTGTGC	1901		
Query 250	AAAAAAGCACAAGTCTAAACAGCTGGCGGCCCGGATCCTGGAAGCTCACCATAACGTAGC	309		
Sbjct 1902	AAAAAAGCACAAGTCTAAACAGCTGGCGGCCCGGATCCTGGAAGCTCACCATAACGTAGC	1961		
Query 310	CCAGATGCCTCTGGTCGAAGCCAAACTGCAGTTCATCCAGGCCTGGCAATCCTTACCTGA	369		
Sbjct 1962	CCAGATGCCTCTGGTCGAAGCCAAACTGCAGTTCATCCAGGCCTGGCAATCCTTACCTGA	2021		
Query 370	GTTTCGGCCTCACCTACTACCTTGTCAGATTTAAAGGAAGCAAAAAAGATGACATCCTGGG	429		
Sbjct 2022	GTTTCGGCCTCACCTACTACCTTGTCAGATTTAAAGGAAGCAAAAAAGATGACATCCTGGG	2081		
Query 430	AGTTGCATACAACAGGTTGATTAGAATCGATGCGGTCACTGGGATACCAGTTACAACGTG	489		
Sbjct 2082	AGTTGCATACAACAGGTTGATTAGAATCGATGCGGTCACTGGGATACCAGTTACAACGTG	2141		
Query 490	GAGATTCGCCAATATGAAGCAGTGGAATGTCAACTGGGAAATCCGGCAGGTGGCAATCGA	549		
Sbjct 2142	GAGATTCGCCAATATGAAGCAGTGGAATGTCAACTGGGAAATCCGGCAGGTGGCAATCGA	2201		
Query 550	GTTTGACCAAAACGTCTCCATCGCATTACCTGCCTAAGTGCAGATTGCAAGATTGTCCA	609		
Sbjct 2202	GTTTGACCAAAACGTCTCCATCGCATTACCTGCCTAAGTGCAGATTGCAAGATTGTCCA	2261		
Query 610	TGAGTACATTGGTGGCTACATCTTCTTGTCACCCGATCCAAGGACCAAAACGAAACGCT	669		
Sbjct 2262	TGAGTACATTGGTGGCTACATCTTCTTGTCACCCGATCCAAGGACCAAAACGAAACGCT	2321		
Query 670	CGATGAGGACCTCTTCCACAAACTGACTGGCGGTGAGGACTGA	712		
Sbjct 2322	CGATGAGGACCTCTTCCACAAACTGACTGGCGGTGAGGACTGA	2364		

Cerebellin 1 (*Cbln1*) synthesized anti-Sense probe with T7 polymerase:

Mus musculus cerebellin 1 precursor protein (Cbln1), mRNA

Sequence ID: [NM_019626.3](#) Length: 2345 Number of Matches: 1

Range 1: 325 to 920 [GenBank](#) [Graphics](#)

▼ Next Match ▲ Previous Match

Score	Expect	Identities	Gaps	Strand
1062 bits(575)	0.0	587/596(98%)	1/596(0%)	Plus/Minus
Query 13	CGAGG-ANCCNGAGAAGGNTGAGTACTTCCAGCCCCCATCAAGTTCCTCCGCTCCNGCT	71		
Sbjct 920	CGAGGAATCCAGAGAAGGTTGAGTACTTCCAGCCCCCATCAAGTTCCTCCGCTCCAGCT	861		
Query 72	TGAGGTATGCTCGGTCGCCTTTCTCCATCTGGATGAGGACGCCGTTGCTGGCGGCCTNNN	131		
Sbjct 860	TGAGGTATGCTCGGTCGCCTTTCTCCATCTGGATGAGGACGCCGTTGCTGGCGGCCTCGC	801		
Query 132	GTGTCACGCTCTTGGTCACCGGCGAAGGCTGAAATCACCGGCCACCCGTTCAACATGAGGC	191		
Sbjct 800	GTGTCACGCTCTTGGTCACCGGCGAAGGCTGAAATCACCGGCCACCCGTTCAACATGAGGC	741		
Query 192	TCACCTGGATGGTCTGTCTGTTGTAGACTTTACCACGTGGAAGTTAAACTGTAGATGC	251		
Sbjct 740	TCACCTGGATGGTCTGTCTGTTGTAGACTTTACCACGTGGAAGTTAAACTGTAGATGC	681		
Query 252	CTTTGCGCGGGGCGATGAAAGTGCTGCGTTCTGAGTCAAAGTTGTTCCCGATGTTCACTA	311		
Sbjct 680	CTTTGCGCGGGGCGATGAAAGTGCTGCGTTCTGAGTCAAAGTTGTTCCCGATGTTCACTA	621		
Query 312	GTACCTGGTCTGAAGTAGATGATCATGGTGCGATTACTCATCTCGGACGGCTCATGGTTGG	371		
Sbjct 620	GTACCTGGTCTGAAGTAGATGATCATGGTGCGATTACTCATCTCGGACGGCTCATGGTTGG	561		
Query 372	TGCTCCTGATGGCAGAGAAAGCCACCTTGGCGCTGCCGAGCGCACAGAGATGCCCAGAG	431		
Sbjct 560	TGCTCCTGATGGCAGAGAAAGCCACCTTGGCGCTGCCGAGCGCACAGAGATGCCCAGAG	501		
Query 432	CAGTGCCCGTAGGGTCAGACGTGGGGTTGGAGTCACACACCACCAGGCACTTGCCCTCCA	491		
Sbjct 500	CAGTGCCCGTAGGGTCAGACGTGGGGTTGGAGTCACACACCACCAGGCACTTGCCCTCCA	441		
Query 492	GTACGATGGGCTCTGTCTATTCTGCCCAGCGGGCTGGGCCTGCCAGCCACGCAGTCCCCA	551		
Sbjct 440	GTACGATGGGCTCTGTCTATTCTGCCCAGCGGGCTGGGCCTGCCAGCCACGCAGTCCCCA	381		
Query 552	ACAGCAGCAGCTCCACGACGCCAGCATCGCGCTCCGGCGCCACCCCGCCTCCC	607		
Sbjct 380	ACAGCAGCAGCTCCACGACGCCAGCATCGCGCTCCGGCGCCACCCCGCCTCCC	325		

Cerebellin 1 (*Cbln1*) synthesized Sense probe with T3 polymerase:

Mus musculus cerebellin 1 precursor protein (Cbln1), mRNA

Sequence ID: [NM_019626.3](#) Length: 2345 Number of Matches: 1

Range 1: 355 to 943 [GenBank](#) [Graphics](#)

▼ Next Match ▲ Previous

Score	Expect	Identities	Gaps	Strand
1085 bits(587)	0.0	588/589(99%)	0/589(0%)	Plus/Plus
Query 26	GCTGGGCGTCGTGGAGCTGCTGCTGTTGGGGACTGCGTGGCTGGCAGGCCCNCCCCGCGG	85		
Sbjct 355	GCTGGGCGTCGTGGAGCTGCTGCTGTTGGGGACTGCGTGGCTGGCAGGCCAGCCCCGCGG	414		
Query 86	GCAGAATGAGACAGAGCCCATCGTACTGGAGGGCAAGTGCCTGGTGGTGTGTGACTCCAA	145		
Sbjct 415	GCAGAATGAGACAGAGCCCATCGTACTGGAGGGCAAGTGCCTGGTGGTGTGTGACTCCAA	474		
Query 146	CCCCACGTCTGACCCTACGGGCACTGCTCTGGGCATCTCTGTGCGCTCCGGCAGCGCCAA	205		
Sbjct 475	CCCCACGTCTGACCCTACGGGCACTGCTCTGGGCATCTCTGTGCGCTCCGGCAGCGCCAA	534		
Query 206	GGTGGCTTTCTCTGCCATCAGGAGCACCAACCATGAGCCGTCCGAGATGAGTAATCGCAC	265		
Sbjct 535	GGTGGCTTTCTCTGCCATCAGGAGCACCAACCATGAGCCGTCCGAGATGAGTAATCGCAC	594		
Query 266	CATGATCATCTACTTCGACCAGGTACTAGTGAACATCGGGAACAACCTTTGACTCAGAACG	325		
Sbjct 595	CATGATCATCTACTTCGACCAGGTACTAGTGAACATCGGGAACAACCTTTGACTCAGAACG	654		
Query 326	CAGCACTTTTCATCGCCCCGCGCAAAGGCATCTACAGTTTTAACTTCCACGTGGTGAAAGT	385		
Sbjct 655	CAGCACTTTTCATCGCCCCGCGCAAAGGCATCTACAGTTTTAACTTCCACGTGGTGAAAGT	714		
Query 386	CTACAACAGACAGACCATCCAGGTGAGCCTCATGTTGAACGGGTGGCCGGTGATTTTCAGC	445		
Sbjct 715	CTACAACAGACAGACCATCCAGGTGAGCCTCATGTTGAACGGGTGGCCGGTGATTTTCAGC	774		
Query 446	CTTCGCCGGTGACCAAGACGTGACACGCGAGGCCGCCAGCAACGGCGTCCTCATCCAGAT	505		
Sbjct 775	CTTCGCCGGTGACCAAGACGTGACACGCGAGGCCGCCAGCAACGGCGTCCTCATCCAGAT	834		
Query 506	GGAGAAAGGCGACCGAGCATACCTCAAGCTGGAGCGGGGGAACCTTGATGGGGGGCTGGAA	565		
Sbjct 835	GGAGAAAGGCGACCGAGCATACCTCAAGCTGGAGCGGGGGAACCTTGATGGGGGGCTGGAA	894		
Query 566	GTA	614		
Sbjct 895	GTA	943		